

Fixed points of Boolean networks with sparse connections

Stav Marcus, Ari M. Turner, Guy Bunin
Technion-Israel Institute of Technology, Haifa, Israel

Bernard Derrida
Collège de France, 11 place Marcelin Berthelot, 75005 Paris, France
Laboratoire de Physique de l'ENS, UMR 8023, CNRS - ENS Paris
- PSL University - SU - Université Paris Cité, Paris, France

We study fixed points of cellular automata with N sites on random sparse graphs. In the large N limit such models are known to exhibit phase transitions, from a “frozen” phase, where at most a finite number of sites fluctuate at long times, to a “fluctuating” phase where a finite fraction of sites fluctuate. We consider several models, calculating the first and second moments of the number of fixed points, and find that these moments remain finite in the large N limit, except at the transitions where they become singular. The singularities can take several forms, including divergence of the mean or variance of the number of fixed points, on one or both sides of the transition. The type of singularity is related to properties of the mean field dynamics or dynamics of the distance between copies of the system. In configuration space, we find that fixed points are organized into clusters, each consisting of sets of fixed points that agree with one another except for on a finite number of sites. In the frozen phase there is only one cluster, while in the fluctuating phase there may be multiple clusters. If there are multiple clusters, the distance between fixed points in different clusters is extensive. We show that the differences within the clusters correspond to local changes near short cycles in the directed graph of connections whose influence is eventually limited. In the frozen phase, we calculate the full distribution of the number of fixed points.

I. INTRODUCTION

Fixed points are objects of prime interest in dynamical systems. One would like to know how many there are, how they are organized in phase space, their stability, their basins of attraction and more. Here we study properties of fixed points (FPs) in cellular automata. Cellular automata are useful models in many fields, for example as models of disordered systems, neural networks, ecological networks, and gene expression networks [1–5].

We consider a set of sites $i = 1, \dots, N$, where the value at site i at time t is a binary variable, $x_i(t) \in \{0, 1\}$. We will also refer to a site i as being “on” or “off” for $x_i = 1, x_i = 0$ respectively. Time is taken to be discrete, and at each time step the sites are updated by the rule $x_i(t+1) = f_i(x_{j_1}(t), x_{j_2}(t), \dots)$, where f_i is a function of the values at a finite number of input sites $x_{j_n}(t)$. Both the set of input sites to i and the function f_i are fixed in time. In the networks considered in the present paper, the connections are chosen randomly and independently, and the functions are also chosen randomly from some ensemble, depending on the choice of model. This kind of system can be represented by a directed graph, with the sites represented as vertices and a link $j \rightarrow i$ if x_j is an input to f_i . We will be interested in the limit where the system has many sites, $N \gg 1$, but the graph of interactions remains sparse, so that the distribution of the number of input sites is independent of N . Due to sparseness, most interactions are “one-way”: if f_i depends on some x_j , then with high probability f_j does not depend on x_i .

Many cellular automata exhibit dynamical phase transitions, from a “frozen” phase, where for sparse random and independent connections, the dynamics of all but possibly a finite number (i.e., independent of N) of variables reach a fixed value, to a fluctuating or chaotic phase, where a finite fraction of the sites change their values indefinitely [6–10]. The Kauffman model, for example, which models the interactions of genes which can regulate one another’s activation state [3, 11], has such a transition to a phase with chaotic dynamics. For a given phase, frozen or fluctuating, the system will reach the corresponding dynamical behavior (fixed in time or fluctuating, respectively) almost surely for any randomly chosen initial conditions. However, the system may have FPs even in the fluctuating phase that can only be reached starting from special initial conditions.

We will be interested in understanding the fixed points in both phases of this phase diagram, and in particular, the probability distribution of the number of fixed points. Besides considering how many fixed points there are we will consider how they are organized in phase space. We will see that the answers are intimately related to the dynamics in the two phases. The idea that this might happen is inspired by considering the Kauffman model, where the number of limit cycles (also known as attractors) diverges in a special way as a function of N at the critical point [12–20]. This suggests that as the critical point is approached, there can be a singularity in the distribution of the number of *fixed points*, since they are just cycles of period 1. We derive formulae relating the statistics of the number of fixed points to dynamics in a precise way (generalizing a formula in Ref. [14]) and we use it to calculate various properties of the number of fixed points. We will also look beyond the Kauffman model in order to see whether there are different

types of behavior in different models. For example, is the behavior universal for all phase transitions from frozen to chaotic phases? The models we consider all consist of networks with a specific type of random one-way connections, similar to Erdos-Renyi directed graphs. An interesting property of this family of models is that the number of FPs is of order 1, except at transitions. Ref. [21] noticed this for a model (which we call the inhibitory model): when this model is considered on an Erdos-Renyi graph with one-way connections, the average number of FPs is independent of the system size, in contrast to the case of a graph where the probability of having an edge from variable i to j is correlated with having an edge from j to i .

In a frozen phase, we will be able to understand the fixed points by reducing the problem to finding FPs for small disconnected parts of the interaction graph, for which it is easy to determine the number of FPs by going through all combinations of values. This method leads to a determination of the full probability distribution for the number of fixed points. In a fluctuating phase, this method does not work; in this phase it is even difficult to count the number of fixed points on a computer, since the only way to find them seems to be to test exponentially many (in N) combinations of the variables. Nevertheless, we will be able to calculate *moments* of the number of fixed points. The method for this is a discrete-variable counterpart of the Kac-Rice technique that applies to systems of interacting *continuous* variables. Such a method has been applied previously to the Kauffman model [14] and in the context of a specific model for ecology [21]. This method gives formulae that determine the expected number of fixed points in terms of a function that describes the evolution of the mean field density for generic initial conditions, as well as generalizations that relate higher moments to the time dependence of correlations between several configurations.

These questions can be generalized to other transitions besides the one from a frozen to a chaotic phase. Besides the Kauffman model, we study three other models (which are of the “regulatory type” studied by [16, 22]) to explore various possible types of behaviors, in particular around the dynamical transition. These are described in the box below. We find that there can be different behaviors in the number of fixed points for the different models, which can be classified into universality classes, and that the behavior is connected to the way the dynamics changes at the transition. In particular, in some cases, which include the Kauffman and the inhibitory model (see Box), the *mean* number of fixed points remains finite at the dynamical transition and is even analytic there, but the *probability* for a fixed point to exist goes to zero, and the *second moment* diverges! How these properties are consistent with each other can be understood from the full distribution of the number of fixed points; on the other hand, the moment formulas give a natural explanation for why the singularity is not seen until the second moment in terms of the relationship between moments and the dynamics.

The variables x_i in all models have two values, denoted by $\{0, 1\}$. All models have one parameter, C , the mean number of incoming edges to each site, with edges from a vertex to itself allowed. The system size (number of sites) is N . The number of fixed points (FPs), Ω , is a random variable that depends on the realization of the disorder. The models considered are:

- Kauffman model: the function determining $x_i(t+1)$ chosen at random, uniformly from functions with appropriate number of inputs.
- Inhibitory model: $x_i(t+1) = 1$ iff for all incoming edges (from j to i) $x_j(t) = 0$.
- Excitatory model: $x_i(t+1) = 1$ iff at least one incoming edge (from j to i) has $x_j(t) = 1$.
- Double excitatory model: $x_i(t+1) = 1$ iff at least TWO of the incoming edges have $x_j(t) = 1$.

This paper is organized as follows. In section 2, we consider the Kauffman model, for which we compute the first and second moments of the number of fixed points. We observe that in the frozen phase, all the fixed points are concentrated in a single cluster, whereas in the fluctuating (i.e. chaotic phase), they are grouped into several clusters at a distance from each other related to the fixed points of the evolution of the overlap fraction. At the transition between the frozen and the fluctuating phase, the second moment of the number of fixed points diverges, growing like $N^{\frac{1}{3}}$ with the number N of sites. In the frozen phase, the analysis of short cycles in the graph allows one to give the physical origin of these results and to obtain the full distribution of the number of fixed points. In section 3, we first show that the approach developed in the previous section to calculate the moments of the number of fixed points can be generalized to other sparse networks of automata. In particular we derive a relation Eq. (16) between the first moment and the evolution $\psi \rightarrow q(\psi)$ of the magnetization (see Appendix A for the derivation), and we discuss the models just listed. We find various differences in the behavior of the moments, corresponding to the difference in their dynamical transitions. In particular, the double excitatory model has a first order transition in its dynamics which causes the first moment to diverge in a different way as a function of $C - C_c$ and N than in models with second order transitions.

II. SOME OF THE MAIN PHENOMENA IN A SINGLE MODEL

A. Kauffman model: definition and dynamical phases

We first introduce some of the main phenomena through the example of one model, the Kauffman model [2]. In the variant of the Kauffman model that we use, one first constructs a random Erdős–Rényi directed graph with a mean of C edges as input connections to each sites. This is done by adding each edge $j \rightarrow i$ to the graph with a probability C/N , including allowing self loops where $j = i$. The inclusion of loops¹ makes results more compact, and does not affect the singular behavior at and near the transitions (see Appendix G for the effects of loops in one model). For large N , which will be assumed throughout, the number k of inputs to a site is therefore approximately a Poisson random variable with probabilities $P_k = e^{-C} C^k / k!$, independently for different sites i . The function f_i that determines $x_i(t+1)$ is chosen at random, uniformly from the 2^{2^k} boolean functions with k inputs (with the convention that if there are no inputs to i , f_i is a constant, and $f_i = 0$ or $f_i = 1$ with equal probability). The connections define a directed graph, with an edge $j \rightarrow i$ if x_j is an input to f_i .

Before discussing FPs, we briefly review some results regarding the dynamical behavior of the model. The model features two dynamical phases [8, 23], depending on C . To see this, we would like to compare the evolution of two configurations of the system initialized with different initial conditions: will they tend to diverge from each other or not?

For this purpose, consider two configurations at time t , $x(t), y(t) \in \{0, 1\}^N$ (where $x = \{x_i\}$ is a binary vector of the values at all sites). Let the overlap fraction ϕ_t be the fraction of sites for which $x_i(t) = y_i(t)$. We calculate ϕ_{t+1} in the limit of large N [23]. Consider the sites i , which can be grouped into two types. The first type are those such that all inputs are equal in x and y , i.e. all $j \rightarrow i$ satisfy $x_j(t) = y_j(t)$, which implies that $x_i(t+1) = y_i(t+1)$. For a site with k input sites, the probability that all inputs are equal is $(\phi_t)^k$, and averaging over k , the fraction of sites of this type is

$$\sum_{k=0}^{\infty} P_k \phi_t^k = e^{C(\phi_t-1)} .$$

The remaining sites are those such that $x_j(t) \neq y_j(t)$ for at least one of the input sites $j \rightarrow i$. In this case, $x_i(t+1)$ and $y_i(t+1)$ are values of f_i for two distinct argument-sets, and since f_i is uniformly sampled from all possible boolean functions, the probability that $x_i(t+1) = y_i(t+1)$ is $1/2$. Taking these two possibilities into account, we find that

$$\phi_{t+1} = q(\phi_t) \tag{1}$$

with

$$q(\phi_t) = e^{C(\phi_t-1)} + \frac{1}{2} [1 - e^{C(\phi_t-1)}] = \frac{1}{2} [1 + e^{C(\phi_t-1)}] . \tag{2}$$

Analyzing this recursion relation, we see that for $C < 2$ it admits only one fixed point, at $\phi = 1$, which is attractive. Therefore, any pair of initial conditions that are different from each other eventually reach an overlap fraction of 1; that is they become equal to one another, apart from a sub-extensive number of sites. Hence all such initial conditions converge to the same final state, up to a subextensive number of sites. This is known as the frozen phase. For $C > 2$, the fixed point at $\phi = 1$ becomes repulsive, and there is another attractive fixed point at some $0 < \phi^* < 1$, given by

$$\phi^* = \frac{1}{2} - \frac{1}{C} W \left(-\frac{C}{2} e^{-C/2} \right) . \tag{3}$$

Here $W(\zeta)$ is the Lambert W-function, defined as the solution to the equation $W e^W = \zeta$. (When $\zeta < 0$ the larger of the two solutions is taken. Several useful facts on this function are collected in Appendix B.) Thus, similar initial conditions (ϕ close to 1) diverge, indicating that this is a fluctuating phase.

B. Moments of the number of fixed points

We now turn to discuss the number of FPs, and whether it changes in a way that reflects the dynamical phase transition just found. An FP is a configuration x such that for all i , $x_i(t+1) = x_i(t)$. The number of FPs is a random variable, denoted throughout by Ω .

¹ Below “loops” refer to edges that connect a vertex to itself, and cycles to refer to closed paths of any length.

1. Calculating the first moment by summing over configurations

One way to calculate moments of Ω is based on the following formula for Ω for a given disorder realization D (i.e., a choice of the connectivity of the graph and the functions f_i):

$$\Omega(D) = \sum_x \mathbb{1}_{x \text{ is FP of } D} .$$

That is, the number of fixed points can be found by summing over all binary vectors $x = \{x_i\}$ a term that is equal to 1 if x is a fixed point and 0 otherwise. The mean number of FPs is thus found by averaging over the different realizations,

$$\langle \Omega \rangle = \sum_D P(D) \sum_x \mathbb{1}_{x \text{ is FP of } D} = \sum_x \sum_D P(D) \mathbb{1}_{x \text{ is FP of } D} . \quad (4)$$

Let us fix the vector x and evaluate the sum over D . For any given x , this sum is just the probability, over the choice of connectivity and of the f_i 's, that x is a fixed point. In other words, if $x(t) = x$, what is the probability that $x(t+1) = x$ as well? Since the output of a random function f_i is equally likely to be 0 or 1, the probability that $x_i(t+1) = x_i(t)$ is $1/2$, and therefore the probability that $x(t+1) = x(t)$ is 2^{-N} . So,

$$\langle \Omega \rangle = \sum_x 2^{-N} = 1 .$$

2. Deriving an expression for the second moment by summing over pairs of configurations

The second moment is given by

$$\langle \Omega^2 \rangle = \sum_D P(D) \left(\sum_x \mathbb{1}_{x \text{ is FP of } D} \right)^2 = \sum_{\{x,y\}} \sum_D P(D) \mathbb{1}_{x \text{ is FP of } D} \mathbb{1}_{y \text{ is FP of } D}$$

Here, x, y are two possible configurations, and we need to calculate the probability over the disorder D that they are both fixed points.

In the following calculation, it will be computationally convenient to work with a slightly different ensemble of networks, which will give the same results in the large N limit. For each site i , one first chooses how many inputs k there should be to this site, and then one chooses the k sites independently from among the vertices in the graph, allowing multiple edges and loops. If the number of inputs is chosen according to a Poisson distribution with a mean C , this will be nearly equivalent to the procedure described in II A when N is large, except for the existence of $O(1)$ multiple edges. Allowing multiple edges can be checked to have no effect on the numbers of fixed points in the limit $N \rightarrow \infty$, however.

Let N_{11} be the number of pairs $(x_i, y_i) = (1, 1)$ at time t , and define similarly N_{01}, N_{10}, N_{00} . Note that $N_{00} + N_{01} + N_{10} + N_{11} = N$. We now calculate the probability q_{11} that for a randomly chosen i , at the next iteration $x_i(t+1) = 1$ and $y_i(t+1) = 1$. Let k be the number of inputs to site i . If x and y are equal on all inputs to f_i , $(x_{j_1}, \dots, x_{j_k}) = (y_{j_1}, \dots, y_{j_k})$, then the values at the next iteration are equal, $x_i(t+1) = y_i(t+1)$, and are both 1 with probability $1/2$. Otherwise, if some inputs are different, then the values $x_i(t+1), y_i(t+1)$ are values of f_i for distinct arguments, so the probability that they are both 1 is $1/4$. Hence, if there are k inputs to site i , the probability that $x_i(t+1) = y_i(t+1) = 1$ is

$$\frac{1}{2} \left(\frac{N_A}{N} \right)^k + \frac{1}{4} \left[1 - \left(\frac{N_A}{N} \right)^k \right] = \frac{1}{4} (1 + \phi^k) ,$$

where $N_A \equiv N_{00} + N_{11}$ and $\phi \equiv N_A/N$ is the fraction of sites that are equal² on x, y . Averaging over the number of inputs k ,

$$q_{11} = \sum_{k=0}^{\infty} P_k \frac{1}{4} (1 + \phi^k) = \frac{1}{4} \left[1 + e^{C(\phi-1)} \right] . \quad (5)$$

² The preceding formula uses the assumption that multiple edges between the same vertices are allowed: each randomly chosen input site has a probability $\frac{N_A}{N}$ that $x = y$ at it, so the probability that this is true for all k input sites is $\left(\frac{N_A}{N}\right)^k$ because the input sites are chosen independently from one another, allowing possible repetitions.

The chances that $x_i(t+1), y_i(t+1)$ have any other pair of values can be found in similar fashion: $q_{00} = q_{11}$, and

$$q_{01} = q_{10} = \sum_{k=0}^{\infty} P_k \frac{1}{4} (1 - \phi^k) = \frac{1}{4} \left[1 - e^{C(\phi-1)} \right]. \quad (6)$$

Now for a site i whose value is 11 at time t (i.e., $(x_i(t), y_i(t)) = (1, 1)$), the chance that it will be fixed after one step is the chance that its value is 11 at time $t+1$, i.e. it is q_{11} . As there are N_{11} such sites, the probability that x, y are both fixed points is $q_{00}^{N_{00}} q_{01}^{N_{01}} q_{10}^{N_{10}} q_{11}^{N_{11}}$. Summing over all possible x, y with the appropriate combinatorial prefactors,

$$\langle \Omega^2 \rangle = \sum_{N_{00}, N_{01}, N_{10}, N_{11}} \frac{N!}{N_{00}! N_{01}! N_{10}! N_{11}!} q_{00}^{N_{00}} q_{01}^{N_{01}} q_{10}^{N_{10}} q_{11}^{N_{11}} \quad (7)$$

where the variables summed over are restricted so that $N = N_{00} + N_{11} + N_{01} + N_{10}$. We simplify this sum by defining $N_A = N_{00} + N_{11}$ and summing over all the N 's with a certain value of N_A . There are two independent variables since $N_{00} + N_{11} = N_A$ and $N_{01} + N_{10} = N - N_A$. Since the $q_{ss'}$ depend only on N_A , the binomial theorem can be used to calculate the sums, giving:

$$\langle \Omega^2 \rangle = \sum_{N_A=0}^N \binom{N}{N_A} q \left(\frac{N_A}{N} \right)^{N_A} (1 - q \left(\frac{N_A}{N} \right))^{N - N_A}, \quad (8)$$

where $q = q_{00} + q_{11} = q(\phi)$ is the same function that appeared in the *dynamics* of the overlap fraction ϕ_t , Eq. (2).

3. Evaluating the second moment using the saddle point method

Since $q(N_A/N)$ depends on N_A , the sum in Eq. 8 is not trivial, so we will approximate it using the saddle point method. At large N , the terms in the sum are equal to $\exp[NA(\phi)]$ within exponential accuracy, with

$$A(\phi) = \phi \ln q + (1 - \phi) \ln(1 - q) - \phi \ln \phi - (1 - \phi) \ln(1 - \phi).$$

This function has either one or two maxima, depending on whether $C < 2$ or $C > 2$, as Fig. 1 illustrates. The sum giving $\langle \Omega^2 \rangle$ is dominated by the contributions near these two maxima,

$$\langle \Omega^2 \rangle = \langle \Omega^2 \rangle_{\text{near}} + \langle \Omega^2 \rangle_{\text{far}},$$

omitting the second term if there is only one maximum. $A(\phi)$ always has one maximum at $\phi = 1$ with $A(1) = 0$. i.e. the contribution is of order 1. As ϕ represents the overlap between the two fixed points x and y , around this maximum they are similar to each other; this is the reason to call this contribution $\langle \Omega^2 \rangle_{\text{near}}$. Let them differ on $n \equiv N - N_A \ll N$ sites. Plugging into Eq. 7 gives:

$$\langle \Omega^2 \rangle_{\text{near}} \approx 1 + \sum_{n=1}^{\infty} \frac{(nC/2)^n}{n!} e^{-nC/2} = \frac{1}{1 + W\left(-\frac{C}{2} e^{-\frac{C}{2}}\right)}. \quad (9)$$

In this expression, W is again the Lambert function. This analytical expression can be derived using a series given in Appendix B.

The second maximum, that exists in the fluctuating phase $C > 2$, turns out to be at ϕ^* that satisfies

$$\phi^* = q(\phi^*),$$

so ϕ^* is precisely the fixed point of the mean-field evolution of the overlap fraction, Eq. (1). This can be deduced by solving $A'(\phi) = 0$ but there is a simpler derivation that applies beyond the Kauffman model that is given in Sec. III A.

At this extremum, as in the maximum at $\phi = 1$, $A(\phi^*) = 0$ and the contribution to $\langle \Omega^2 \rangle$ is $O(1)$. The sum near this extremum can be approximated by an integral—the usual Gaussian saddle point approximation is sufficient. This, with the help of $\phi^* = q(\phi^*)$, whose solution is Eq.(3), gives

$$\langle \Omega^2 \rangle_{\text{far}} = \frac{1}{|1 - q'(\phi^*)|} = \frac{1}{1 - C(\phi^* - 1/2)} = \frac{1}{1 + W\left(-\frac{C}{2} e^{-\frac{C}{2}}\right)}. \quad (10)$$

(See III A for the derivation.) Fig. 1 shows the final result for $\langle \Omega^2 \rangle$. In both phases, $\langle \Omega^2 \rangle$ is finite, namely does not scale with N , except at $C = 2$ where this number diverges.

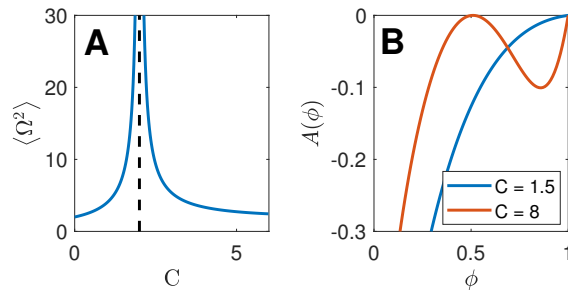


Figure 1. (A) $\langle \Omega^2 \rangle$ for the Kauffman model. The dashed vertical line marks the transition at $C = 2$. (B) The function $A(\phi)$ for two values of C , below and above the transition. It shows the saddle point contributions to $\langle \Omega^2 \rangle$ at $\phi = 1$ for both values of C , and for $C > 2$ the contribution at $0 < \phi^* < 1$.

4. The second moment and the organization of FPs in configuration space

Consider now whether some of the fixed points of a given random cellular automaton of the Kauffman model are similar to one another. This can be investigated by considering the expression for $\langle \Omega^2 \rangle$. In the frozen phase, $C < 2$, the only maximum of $A(\phi)$ is at $\phi = 1$, and the only contribution to $\langle \Omega^2 \rangle$ is $\langle \Omega^2 \rangle_{\text{near}}$. Thus, all pairs of FPs are at a finite distance from each other (finite number of sites where $x_i \neq y_i$). The expression in Eq. (9) simplifies (see Appendix B) to

$$\langle \Omega^2 \rangle = \frac{1}{1 - C/2} \quad (C < 2) \quad (11)$$

This simple result is derived in a different way in Sec. II C.

Throughout the fluctuating phase, $C > 2$, the contributions to $\langle \Omega^2 \rangle$ are non-zero from both $\langle \Omega^2 \rangle_{\text{near}}$ and $\langle \Omega^2 \rangle_{\text{far}}$, so there are pairs of fixed points at a finite distance or at an extensive distance from each other. In other words, FPs are arranged in clusters of fixed points at a finite distance from each other, while fixed points in different clusters are at an extensive distance from each other. Both contributions are the same by Eqs. (9), (10), giving

$$\langle \Omega^2 \rangle = \frac{2}{1 + W\left(-\frac{C}{2}e^{-\frac{C}{2}}\right)}.$$

Approaching the transition from above, $C \rightarrow 2^+$, $\langle \Omega^2 \rangle \approx \frac{2}{C/2-1}$. So $\langle \Omega^2 \rangle$ diverges with the same exponent as for $C \rightarrow 2^-$, but with a factor of 2 difference in the prefactor.

When C is close to 2, the sum in Eq. (8) is dominated by values of N_A that are close to N , but $N - N_A$ is not of order 1 as it is when C is below 2 by a finite amount. Thus, we write $N_A = N(1 - u)$ and find that Eq. (8) becomes, for u small and C close to 2:

$$\langle \Omega^2 \rangle \simeq \frac{\sqrt{N}}{2\pi} \int_0^1 \frac{du}{\sqrt{u}} \exp\left[-\frac{Nu(C-2-2u)^2}{8}\right] \simeq N^{\frac{1}{3}} f(N^{\frac{1}{3}}(C-2))$$

where $f(z) = \int_0^\infty \frac{dv}{\sqrt{2\pi v}} \exp\left[-\frac{v(z-2v)^2}{8}\right]$. In particular, at the transition, i.e., for $z = 0$, one gets $\langle \Omega^2 \rangle = \frac{2^{\frac{2}{3}}}{\sqrt{\pi}} \Gamma\left(\frac{7}{6}\right) N^{\frac{1}{3}} \simeq .83N^{\frac{1}{3}}$. This result is correct whether C is above or below 2, and one can see that it matches the $C - 2$ dependence found above outside the critical region.

C. Distribution of number of FPs in the frozen phase, based on short cycles

In Sec. II B we saw that in the frozen phase, $C < 2$, all fixed points are at a finite distance from each other. We also found an expression for $\langle \Omega^2 \rangle$ as an infinite sum, which reduced to $1/(1 - C/2)$, see Eq. (11). Here we explain the origin of these similar fixed points, and obtain the full distribution $P(\Omega)$ in the frozen phase.

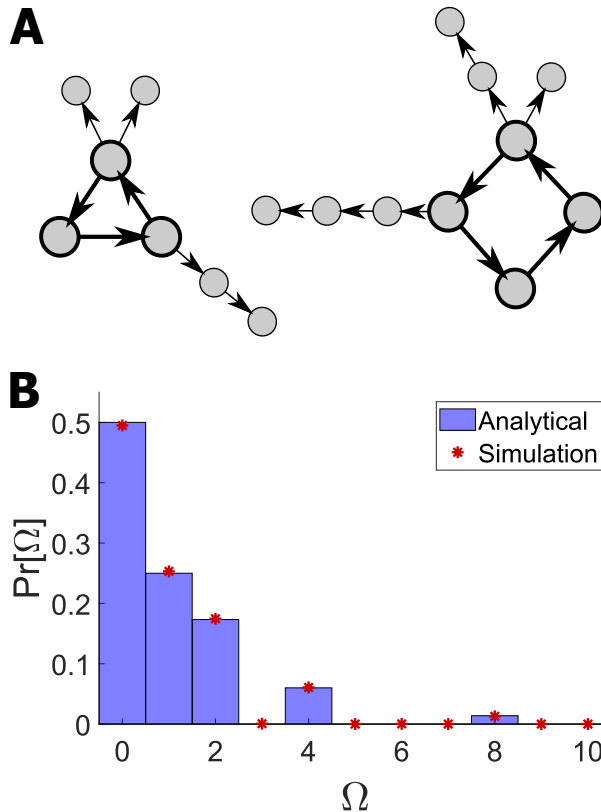


Figure 2. **Distribution of the number of FPs in the frozen phase.** (A) Example of the subset I , of sites on which assignments change between FPs in the frozen phase. (B) The final $P(\Omega)$, theory (blue bars) against exhaustive searches after graph simplification (red points). Both panels are obtained by first applying the simplification algorithm (see main text) for instances with $C = 1.5$ and $N = 5000$ sites.

1. The graph structure of sites differing between FPs

Suppose we have two FPs, x, y , that differ from each other on a finite subset I of sites. The graph on I has a special structure, illustrated in Fig. 2(A). To see the structure, start from some site $i \in I$. Since $x_i \neq y_i$, there must be a site $j \rightarrow i$ for which $x_j \neq y_j$, meaning that $j \in I$. This way, one can continue to go upstream, following the inputs to j and so on, to create a string of sites in I . Since I is finite, this string must close on itself after a finite number of steps, so there must be a finite directed cycle in I . In random sparse graphs, cycles of finite length are distant from each other (the distance between two finite cycles increases with N [24]), and so the connected component of site i can include only a single cycle, possibly with trees emanating from the sites on the cycle. There may be a finite number of such connected components of I . Thus I has a specific structure: it is made up of a finite number of cycles with trees emanating from them.

In the frozen phase, any two FPs were found above to be at a finite distance from one another, so the set where two such FPs differ always has the structure of disconnected cycles with emanating trees. The fact that in this phase any two distinct FPs are only different on a finite number of sites, with this connectivity, suggests that for any random Kauffman network there is a specific subset of sites which can differ between different FPs, also made up of disjoint cycles with trees emanating from them, while all other sites are the same in all FPs.

Now we can justify this last assumption. First, we show that for typical sites, that are located in a locally tree-like neighborhood, the value that they may take in an FP is unique. We first provide numerical evidence for this. We use an algorithm that simplifies an instance of the Kauffman model, iteratively finding sites and edges that have the same value in all FPs and removing them. We then analyze this algorithm's dynamics to show that indeed most sites have unique values in all FPs. (They form the “stable core”, [12, 18, 19, 25, 26].) The algorithm makes the following modifications to the system:

(1) The value x_i of a site i that has no inputs has a unique value, in all FPs. The site can then be removed, along with the edges outgoing from it. The functions downstream are reduced to functions of fewer variables, by fixing the value of x_i .

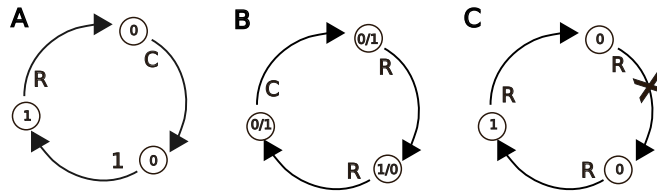


Figure 3. Examples of cycles that may affect the FP number in the Kauffman model. The functions are labeled on the arrows: The constant function $f(x) = 1$ is labeled as 1; the “copy” function $f(x) = x$ as “C”, and the “reverse” function $f(x) = 1 - x$ as “R.” (A) A cycle with any constant function has a unique fixed point and is removed from the reduced graph: in this example the function 1 is constant so, starting from it, all the sites along the cycle are determined. (B) A cycle with two fixed points. (C) A cycle with no consistent fixed points.

(2) When there is an edge $j \rightarrow i$ such that the function f_i giving x_i does not depend on the value of x_j , the edge can be removed.

These modifications do not change the number of fixed points of the system. They are applied alternately until there are no vertices or edges to which they can be applied. Running this algorithm shows that instances of large systems can be reduced significantly, and for large N the outcome is of the form described above for I : a few cycles, with downstream trees emanating from the cycles, see Fig. 2(A). The difference I between two FPs will include some or all of the connected components found this way. The simplified graphs can be exhaustively searched to count FPs, which is used to find the probability distribution for Ω , and thus to test the theory below.

The analysis of the algorithm proceeds by defining auxiliary dynamics describing how the number of sites that are removed changes at each step. In this dynamics, each site takes the values 0 or 1 once its value has been determined, and u when its value is yet unknown, or varies between FPs. It is shown that in the frozen phase the fraction of sites with value u goes to zero when $t \rightarrow \infty$. The detailed analysis is given in Appendix D.

This suggests that all but $O(1)$ sites have uniquely determined values (which is seen in the simulations). If a site remains in the simplified graph, at least one of its inputs must also be in the simplified graph. As for I it follows that the simplified graph is made up of finite cycles plus sites downstream from them.

2. The number of FPs on a finite cycle

We can now count the number of fixed points, by considering only the number of FPs in the simplified graph. We will find that it is related to the number of short cycles of certain types. (Ref. [22] found bounds on the number of fixed points in the fluctuating phase using cycles in a similar way.) Although the simplified graph is made up of cycles with trees emanating from them, we only need to evaluate the number of FPs that can be assigned to the cycles, as once the values on the cycle are given, the assignments of the downstream trees is uniquely determined.

For a cycle of length n , denote by $i_1 \rightarrow i_2 \rightarrow \dots \rightarrow i_n \rightarrow i_1$ the indices of the sites along the cycle. After the reduction of the system described in the previous section, there are reduced functions $x_{i_k} = f_{i_k}^{\text{red}}(x_{i_{k-1}})$ that must be satisfied at an FP. They are random functions of one binary variable, since they are obtained by reducing the original many-variable functions by fixing all but one input of the function. The inputs that are fixed come from random sites in the system, that are therefore almost surely not in the simplified graph, and therefore have fixed values 0 or 1 with equal probability and independently between them.

There are several cases depending on what the functions along the cycle are, see Fig. 3. First, notice that the cycles cannot have any reduced function that is a constant, as in Fig. 3A. If one of the $\{f_{i_k}^{\text{red}}\}$ is a constant function, then there is a unique FP assignment to the cycle: because $f_{i_k}^{\text{red}}$ is a constant function, the value at site i_k is fixed, and from there the rest of the sites are fixed as well by following the cycle. In this case, the cycle has uniquely determined values and it is not in the simplified graph.

For the cycles that do belong to the reduced graph, there are either 0 or 2 fixed-point assignments. To find them, one can start by assigning $x_{i_1}^* = 1$, and from there obtaining the values $x_{i_2}^*, \dots, x_{i_n}^*$ along the cycle. There are no assignments if $x_{i_1}^* \neq f_{i_1}^{\text{red}}(x_{i_n}^*)$ (that is, if the cycle does not “close on itself”); the probability of this is $1/2$. Otherwise there are two FP assignments because the values on the entire cycle can be flipped, as all functions are either “copy” or “reverse”. So the number of FPs for the network is zero if the reduced graph has any cycle without FPs; and otherwise, the number of FPs is 2^k , where k is the number of cycles in the reduced graph. Thus determining the full distribution for Ω reduces to finding the distribution of k and the probability to have a cycle with 0 fixed points.

3. The full FP number distribution in the frozen phase

We consider a cycle in the graph describing the system, of length n . What is the probability that it is in the reduced graph, and that it has 0 or 2 fixed points? Every site that gives an input to the cycle will be eliminated during the reduction process³, so the values of these inputs are fixed. So we can consider the cycle with all the reduced one-variable functions along it. If any function is constant, the cycle will also be eliminated. Each function along a cycle is sampled with equal probability from the four functions $\{0, 1\} \rightarrow \{0, 1\}$, two of which are constant, so the probability that there are no constant functions is 2^{-n} . Supposing that this is the case, the conditional probabilities for 0 or 2 fixed points are both $1/2$. So in total the probabilities are

$$P(\Omega_n = 0) = P(\Omega_n = 2) = 2^{-n-1} ,$$

where Ω_n represents the number of FPs for this cycle. These alternatives for different cycles are independent as the cycles are far from each other.

Now in terms of C , the mean number of directed cycles of length n is $\lambda_n = C^n/n$, and this number is Poisson distributed. (This also applies to a graph where the number of incoming edges is fixed to be exactly C and the number of outgoing edges may fluctuate, as the Kauffman model is often defined; hence the results below also apply to this version of the Kauffman model.) If there is at least one short cycle in the reduced graph with no FP assignment, then there is no FP assignment for the entire system. The probability that all

$$\sum_{j=0}^{\infty} \frac{e^{-\lambda_n}}{j!} \lambda_n^j (1 - 2^{-n-1})^j = e^{-(C/2)^n/(2n)}$$

where j represents the number of cycles of length n . So the probability that all cycles of *any* length n have FP assignments is

$$\Pr[\Omega \neq 0] = \prod_{n=1}^{\infty} e^{-(C/2)^n/(2n)} = (1 - C/2)^{1/2} .$$

This is the probability that there is at least one FP of the system.

Now to determine the distribution of the number of fixed points, we must consider how many cycles allow different choices. The number of cycles of length n with 2 FP assignments is Poisson distributed with mean $\lambda_n P(\Omega_n = 2)$, and so k , the total number of cycles that have 2 FP assignments, is Poisson distributed with mean

$$m_2 = \sum_{n=1}^{\infty} \lambda_n P(\Omega_n = 2) = \sum_{n=1}^{\infty} \frac{C^n}{n} 2^{-n-1} = -\frac{1}{2} \ln(1 - C/2)$$

When there are k such cycles, and no cycles without an FP, there are 2^k FPs of the entire system.

This gives the probability distribution: The probability for 2^k fixed points is

$$\begin{aligned} \Pr[\Omega = 2^k] &= \Pr[\Omega \neq 0] \Pr[k \text{ cycles with 2 FPs}] \\ &= (1 - C/2)^{1/2} \frac{m_2^k}{k!} e^{-m_2} = \frac{1 - C/2}{2^k k!} \left[\ln \left(\frac{1}{1 - C/2} \right) \right]^k \end{aligned}$$

where in the first equality the probability factorizes due to properties of Poisson distributions⁴. Together

$$P(\Omega) = \begin{cases} 1 - (1 - C/2)^{1/2} & \Omega = 0 \\ (1 - C/2)^{1/2} \frac{1}{2^k k!} \left[\ln \frac{1}{1 - C/2} \right]^k & \Omega = 2^k, k \geq 0 \\ 0 & \text{otherwise} \end{cases} \quad (12)$$

³ A site that is not eliminated must have a cycle upstream and close to it, so such a site would have to be close to two cycles. This does not occur in a sparse random graph.

⁴ For each cycle length n , the number of cycles with 0 or 2 FPs are independent Poisson random variables. Therefore, the number of cycles of any length with zero FPs, which sets $\Pr[\Omega \neq 0]$, is independent of the number of cycles with 2 FPs, which sets $\Pr[k \text{ cycles with 2 FPs}]$.

This distribution is in excellent agreement with results of an exhaustive search for FPs, see Fig. 2(B), in which the simplifying algorithm described above is applied to the graph and then all fixed points are found using an exhaustive search on the simplified graph.

From $P(\Omega)$, the r -th moment can be calculated:

$$\langle \Omega^r \rangle = (1 - C/2)^{1-2^{r-1}} \quad (13)$$

which agrees with the calculation above for $\langle \Omega \rangle$ and $\langle \Omega^2 \rangle$ in the frozen phase, Eq. (11).

Note that, approaching the transition at $C = 2$ from below, one obtains that $\langle \Omega^r \rangle$ for $r \geq 2$ diverges while the first moment remains constant at the transition, while the probability of having an FP goes to zero as $P(\Omega > 0) \sim (2 - C)^{1/2}$. This is possible because the number of fixed points grows exponentially with the number of cycles. The value of $\langle \Omega^r \rangle$ is dominated by contributions where the number of cycles with two possible fixed point assignments is $2^{r-1} \log \frac{1}{2-C}$. This is very unlikely (typically there are about $\log \frac{1}{C-2}$ cycles), but the number of fixed points is very big when it happens.

4. The structure of FPs in the fluctuating phase

Some of the ideas just considered are also helpful for understanding fixed points in the fluctuating phase, although they do not lead to the full distribution function. The two contributions to $\langle \Omega^2 \rangle$, namely $\langle \Omega^2 \rangle_{\text{near}}$ and $\langle \Omega^2 \rangle_{\text{far}}$, count pairs of fixed points with a full overlap or a partial overlap of ϕ^* respectively. These contributions can be understood by partitioning fixed points into clusters, where each cluster is made of fixed points that differ from each other only at a finite number of points, on and near cycles. Ω^2 equals the number of pairs of fixed points (counting a pair (i, j) and (j, i) separately and also counting (i, i) as a pair). If there are p clusters, and n_i fixed points in the i^{th} cluster, then $\Omega^2 = \sum_{i=1}^p n_i^2 + 2 \sum_{i=1}^p \sum_{j=1}^{i-1} n_i n_j \equiv (\Omega^2)_{\text{near}} + (\Omega^2)_{\text{far}}$. The means of the two terms give the contributions $\langle \Omega^2 \rangle_{\text{near}}$ and $\langle \Omega^2 \rangle_{\text{far}}$ found above, since $\langle \Omega^2 \rangle_{\text{near}}$ represented the part of the sum (8) near the saddle point with $\psi_{01} = \psi_{10} = 0$, corresponding to pairs of fixed points that overlap at almost all the sites, while the latter includes the rest of the pairs of fixed points.

In the frozen phase, there is only one cluster, and above we were able to find the full distribution function for the number of fixed points in this cluster. In the fluctuating phase, the fixed points in each cluster still differ from one another by the values along cycles and trees extending from the cycles (for the same reason as in the frozen phase). However, it is not easy to find *which* cycles can be changed in this way. This is because the reduced version (using the reduction algorithm from above) of the graph contains an extensive number of sites and thus many cycles, which can be close to one another or overlap. Nevertheless, since $\langle \Omega \rangle$ is finite, there must be only finitely many FPs in each cluster. The reason is probably that there are only finitely many cycles that can be changed without destabilizing the whole FP. We also do not know the full probability distribution for the number of distinct clusters. Because these phenomena are harder to understand, we do not know the full probability distribution in the fluctuating phase.

The calculation of $\langle \Omega^2 \rangle$ gives one interesting result about the clusters: since $\langle \Omega^2 \rangle_{\text{far}}$ is dominated by one saddle point, where all pairs of fixed points overlap at a fraction ϕ^* of the sites, any two fixed points from distinct clusters have the same distance from one another, $1 - \phi^*$.

III. DIFFERENT TYPES OF TRANSITIONS, AND HOW THEY AFFECT THE FIXED POINTS

We will now consider the other models shown in the box above, which exhibit a range of phenomena. These models can be understood more intuitively if we consider sites at 0 and 1 as being “off” and “on” respectively. To derive their properties, we will use both of the methods from the previous section, the geometrical method based on cycles (which gives a full distribution function in the frozen phases) and the evaluation of moments, which gives less complete information, but works in any phase and makes an interesting connection between the dynamics and the number of fixed points. We will first discuss this connection.

We consider mostly the first moment. In the Kauffman model, the first moment is very simple (always equal to 1), so we analyze mainly the second moment.

A. Formula for Fixed Points based on Dynamics

Here we will give a formula for the moments of Ω in any general cellular automaton. Consider a model with binary variables, with random sparse connections as above. For an assignment x of values for the N sites, let ψ be the

fraction of sites for which $x_i = 1$, which we will below call the magnetization. The time dependence of ψ_t is described by a dynamical equation when N is large,

$$\psi_{t+1} = q(\psi_t), \quad (14)$$

aside from small fluctuations. Here q is some function that can be obtained for each model, given its ensemble of functions. Notice that $q(\psi_t)$ can also be interpreted as the probability that a random function from the ensemble takes 1 as its value for inputs chosen randomly from among all the sites.

The first moment $\langle \Omega \rangle$ can be related to q , (see also Ref. [14]) following a derivation similar to that in Sec. II B, see Appendix A. Begin with Eq. (4). The sum over D is the probability that x is a fixed point. If the value of a site is equal to 1, then the probability that it is fixed (for one step of evolution) is $q(N_1/N)$, because the condition that it is fixed means that the function assigned to it comes out to equal 1. Similarly, if its value is 0, the probability that this configuration is fixed at the site is $1 - q(N_1/N)$. Thus the expected number of fixed points is

$$\langle \Omega \rangle = \sum_{N_1=0}^N \binom{N}{N_1} q(N_1/N)^{N_1} (1 - q(N_1/N))^{N-N_1}. \quad (15)$$

To evaluate this sum by the saddle point method, we write the terms to exponential accuracy as $e^{A(\psi)N}$, where $\psi = N_1/N$ and $A(\psi) = \psi \ln \frac{q(\psi)}{\psi} + (1 - \psi) \ln \frac{1-q(\psi)}{1-\psi}$. Solving $A'(\psi) = 0$ algebraically, in order to find the saddle points, is not possible for a general function q ; however following [14], we can argue that as $-\ln x$ is convex, Jensen's inequality implies $A(\psi) \leq \ln[\psi \frac{q(\psi)}{\psi} + (1 - \psi) \frac{1-q(\psi)}{1-\psi}] = 0$. This maximal possible value, $A = 0$, is attained only when $\frac{q(\psi^*)}{\psi^*} = \frac{1-q(\psi^*)}{1-\psi^*}$, or $\psi^* = q(\psi^*)$, where ψ^* is the position of the maximum⁵. Such a value is a fixed point of the dynamics of the *magnetization* (a different concept from the fixed points that we have been studying, which are fixed point *configurations* of the automaton). It makes sense that the main contributions to $\langle \Omega \rangle$ come from fixed points of q , since in order for a configuration to be an FP, i.e., for *each* site's value not to change in time, the magnetization ψ must a fortiori be independent of time, which means that it is a fixed point of $\psi \rightarrow q(\psi)$. As $q(\psi)$ is a function $[0, 1] \rightarrow [0, 1]$, this must have at least one solution.

Since $A(\psi^*) = 0$ at the extrema and the contribution to the sum is $e^{A(\psi)N}$ (apart from possibly a power of N), the number of fixed points neither grows nor decays exponentially with N . The sum of Eq. (15) in the vicinity of an extremum can be approximated by a Gaussian integral when $\psi^* \notin \{0, 1\}$, giving

$$\frac{1}{|1 - q'(\psi^*)|}; \quad (16)$$

see Appendix A. In particular the expected number of fixed points approaches a finite limit when $N \rightarrow \infty$, unless $q'(\psi^*) = 1$. (The formula for the *second moment* in the Kauffman model has the same form (Eq. (8)) but this is special for the Kauffman model because in it the sum for the second moments, Eq. (7), can be replaced by a sum over just the overlap fraction, Eq. (8), that has the same form as the general expression for the first moment. In the appendices the more general sums are evaluated.)

The second moment $\langle \Omega^2 \rangle$ can be calculated in a similar way from Eq. (7), with the functions q_{00}, \dots, q_{11} describing the dynamics of two configurations. That is, let $\psi_{00} = N_{00}/N$ etc. The functions $q_{00}, q_{10}, q_{01}, q_{11}$ give the time dependence of these variables, e.g. $\psi_{00}(t+1) = q_{00}(\psi_{11}(t), \psi_{10}(t), \psi_{01}(t), \psi_{00}(t))$. The extrema are solutions to simultaneous equations $\psi_{ij} = q_{ij}(\psi_{ij})$ where $i, j \in \{0, 1\}$. The contribution to $\langle \Omega^2 \rangle$ from an extremum away from the boundary of the domain of physical values of ψ_{ij} can be found by a Gaussian approximation, generalizing Eq. (16). There is always at least one solution: this is when the two copies are the same, and $\psi_{01} = \psi_{10} = 0$, $\psi_{11} = \psi^*$, $\psi_{00} = 1 - \psi^*$.

The Gaussian approximation will break for $\langle \Omega \rangle$ for extrema at $\psi^* = 0$ or $\psi^* = 1$, and it will break for $\langle \Omega^2 \rangle$ for extrema on the boundary of the domain of ψ_{ij} 's. In this case one has to evaluate a sum (much like the contribution to $\langle \Omega^2 \rangle_{\text{near}}$ in the Kauffman model), since then the terms of Eqs. (7) or (15) are not smooth enough to be approximated by integrals. The sums can still be expressed in terms of the derivatives of q at the saddle point (see Appendix C), and for some of the models studied here they can be expressed in terms of the Lambert function like for the Kauffman model.

From this dynamical point of view, where the moments are written entirely in terms of the function $q(\psi)$ and its analogues for several copies of a system, there are different universality classes for the behavior of Ω that are

⁵ There can be local maxima with smaller values of A , which would not be fixed points of q . Their contributions to $\langle \Omega \rangle$ can be neglected compared to contributions near the points where $A = 0$, if there are any such points. In fact such points always exist because q is continuous and maps the interval $[0, 1]$ into itself, which implies that $q(\phi) = \phi$ has a solution.

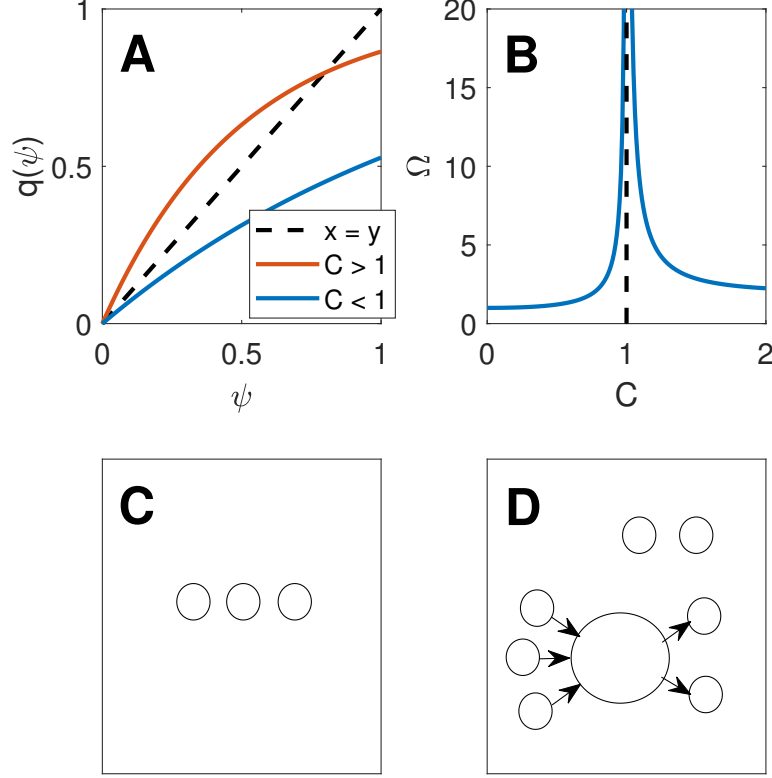


Figure 4. **The excitatory model.** (A) The function $q(\psi)$ for different values of C , above and below $C_{\text{crit}} = 1$. (B) The first moment $\langle \Omega \rangle$. (C) SCCs in the phase $C < C_{\text{crit}}$. Each circle denotes an SCC, each containing a finite number of sites. (D) SCCs in the phase $C > C_{\text{crit}}$ include a giant SCC comprised of a finite fraction of the sites (large circle), and possibly a finite number of SCCs with a finite number of sites (small circles). They may be disconnected from the giant component, or with directed paths to or from it. Arrows denote paths of links between the SCCs.

determined by the type of bifurcation transition that occurs in the graphs of these functions, as described in several examples in the remainder of this section.

We have seen that all fixed point configurations have a magnetization that is very close to a fixed point of the magnetization dynamics, $\psi^* = q(\psi^*)$ (almost surely). This is intuitively reasonable, but it allows something surprising to happen: If ψ^* is an *unstable* fixed point of q there are still FPs nearby. Since unstable fixed points still have a finite value of $q'(\psi^*)$ (one that is > 1), Eq. (16) shows that there are $O(1)$ FPs associated with them. There are examples of this in all the models considered below. For example, in the Inhibitory model, Sec. III D, simulations with parallel dynamics show that in the non-frozen phase the solution to $\psi = q(\psi)$ is dynamically unstable towards a 2-cycle, yet the mean number of FPs is not 0 because a contribution to $\langle \Omega \rangle$ is produced by the unstable solution.

When the $\vec{\psi}^*$ at the saddle point does not have any components that are equal to zero, the sum becomes smooth so it can be approximated by an integral, and the integral is a Gaussian integral: The expression has the form: $e^{NA(\vec{\psi})}$ times a coefficient that is a power of N . Expanding gives $A = A(\vec{\psi}^*) + \frac{1}{2} \frac{\partial^2 A}{\partial \psi_{ij} \partial \psi_{rs}} (\psi_{ij} - \psi_{ij}^*) (\psi_{rs} - \psi_{rs}^*)$ because there is no first order term. The exponential decays when the n_{ij} change by an amount $\sim \sqrt{N}$, so there are many terms in the sum over n_{ij} within this range, and it can be approximated by an integral. But when the maximum is at the edge of the range of integration, it could be possible that the first derivative is nonzero, and then the sum would decay on a scale of order 1, and it cannot be approximated by an integral. (It turns out that A does not even have a Taylor series expansion around 0 in this case. See appendix A.)

B. The Excitatory model

The model of this section and the next have simpler dynamical transitions than the Kauffman model: the mean-field dynamics changes rather than the system going from a frozen to a fluctuating state with the same mean-field values. This is reflected even in the first moment of the number of fixed points. The excitatory model is defined by the dynamical rule: $x_i(t+1) = 1$ iff at least one incoming edge $j \rightarrow i$ has $x_j(t) = 1$. The magnetization ψ satisfies $\psi_{t+1} = q(\psi_t)$ with $q(\psi_t) = 1 - e^{-C\psi_t}$. The value $\psi^{(1)} = 0$ is a fixed point of this equation, for all C . For $C > C_{\text{crit}} \equiv 1$ there is another fixed point at some $\psi^{(2)} > 0$.

The mean number of FPs $\langle \Omega \rangle$ diverges on both sides of the transition C_{crit} , see Fig. 4(B). The calculation is given in Appendix E. This can be seen from the graph of $q(\psi)$ in Fig. 4 (A). At C_{crit} , where one fixed point bifurcates into 2, the line $y = x$ is tangent to the graph of q , so the slope is 1 and Eq. 16 diverges. (This argument applies actually only above C_{crit} to the nonzero saddle point, $\psi^{(2)}$, since Eq. (16) assumes $\psi^* \neq 0, 1$, but the other contributions also diverge.)

This model is interesting because the FPs have a geometrical interpretation, allowing one to understand and calculate $P(\Omega)$ on both sides of the transition, and to understand why there are two clusters of fixed points. At an FP, if there is an edge $j \rightarrow i$ then $x_j \leq x_i$, namely $x_i = 1$ if $x_j = 1$. This then applies to any path between sites: if there is a path from j to i , $j \rightarrow \dots \rightarrow i$, then $x_j \leq x_i$ at an FP; i.e., if a site must be on if any site upstream of it is. Now consider the strongly connected components (SCCs) of a directed graph. An SCC is a subset of vertices for which there are directed paths in both directions between all vertices in the subset. From the above, at an FP the value x_i must be equal for all sites i in an SCC: the entire SCC is either off or on. Next, SCCs admit a partial ordering: if there is a path from one SCC to another (but not in both directions, otherwise they would be the same SCC), for a site j in the upstream SCC and a site i in the downstream one, there is a path $j \rightarrow \dots \rightarrow i$ and so at an FP $x_j \leq x_i$. In other words, if an SCC is on, then all of the downstream SCCs will also be on.

The transition at C_{crit} is due to the percolation transition which changes the geometry of the SCCs, with the appearance of an SCC giant component, see Fig. 4(C,D). Below the transition there are only a finite number of SCCs, all of finite size, which are precisely the short directed cycles in the graph, and which are disconnected from one another (with probability 1). Each short cycle can be assigned either 0 or 1, giving several fixed points. All sites that are not downstream from a cycle must be off at a fixed point⁶, and so these FPs will be associated with the magnetization $\psi^{(1)} = 0$. Above the transition there is also a giant SCC, comprised of a finite *fraction* of the sites. This means that there are two clusters of FPs, corresponding to whether the giant component is off or on; the latter type of fixed point is associated with the saddle point $\psi^{(2)} > 0$, since the number of sites with value 1 is extensive for such a fixed point. This picture allows to calculate $P(\Omega)$, see details in Appendix E.

The dynamics of this model is simpler than in the Kauffman model because even when $C > C_{\text{crit}}$ it is not fluctuating; the dynamics just changes: below C_{crit} every state is attracted to frozen states where $\psi \approx \psi^{(1)} = 0$ (the small SCCs may be on) while above C_{crit} it is attracted to the states near $\psi^{(2)}$ with a giant SCC, which are also frozen states. In addition, there are still fixed points near $\psi^{(1)} = 0$, which have small basins of attraction (as they require all SCCs upstream of the giant SCC to be at 0).

C. The Double excitatory model

The double-excitatory model is defined by the dynamical rule: $x_i(t+1) = 1$ iff at least *two* of the incoming edges have $x_j(t) = 1$. This captures situations where there is a barrier for a transition, such as a voltage threshold for a neuron to fire.

The magnetization ψ satisfies $\psi_{t+1} = q(\psi_t)$ with $q(\psi_t) = 1 - e^{-C\psi_t} (C\psi_t + 1)$, see Fig. 5(A). The value $\psi^{(1)} = 0$ is a fixed point for all C . For $C < C_{\text{crit}} \approx 3.35$, the solution $\psi^{(1)} = 0$ is unique. At C_{crit} there is a transition where two additional fixed points appear, $\psi^{(2)} < \psi^{(3)}$. This is a first order transition, in the sense that these fixed points are not close to $\psi^{(1)}$ at C_{crit} ; the graph of $y = q(x)$ has a convex part that first meets $y = x$ in a new pair of points when C increases above C_{crit} (see Fig. 5 A). $\psi^{(2)}$ is unstable, so the dynamics reaches either of the stable FPs, $\psi^{(1)}$ or $\psi^{(3)}$, depending on initial conditions. This transition is related to a transition for an undirected graph, where a “3-core” appears when the average degree of the vertices is increased (a subgraph where each vertex has at least 3 neighbors)[27].

The first moment $\langle \Omega \rangle$ is calculated with the same technique as above, see Appendix F. The result is plotted in Fig. 5(B). At $C < C_{\text{crit}}$ just one term, exactly at $\psi^{(1)} = 0$, gives the total number of fixed points $\langle \Omega \rangle = 1$. (If $N_1 > 0$,

⁶ If a site is on at an FP, then at least one site upstream from it must also be on. Iterating this gives a sequence of sites that are on, and the sequence must close into a cycle eventually.

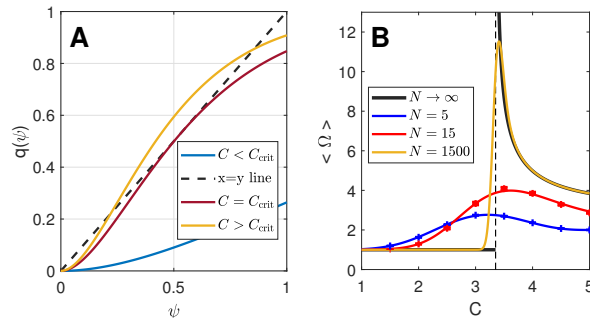


Figure 5. **The double-excitatory model.** (A) The saddle-point function for $\langle \Omega \rangle$ as a function of ψ , at $C = 2, 3.35, 4$. (B) $\langle \Omega \rangle$ for the Double Excitatory model (black curve), and finite- N behavior. Solid curves are calculated from an exact evaluation of $\langle \Omega \rangle$ when expressed as a sum, and crosses (with 1SE error bars) are the results of exhaustive searches at $N = 5, 15$, each averaged over 1000 disorder realizations. Dashed line: transition at C_{crit} .

the terms are smaller by at least $\frac{1}{N}$.) The reason why there are no other FPs near the FP where all sites are off, is that the double excitatory condition implies that each site that is on belongs to at least two cycles of sites that are also on. This cannot happen for a finite subset of the sites in an Erdős–Rényi graph when $N \rightarrow \infty$. (This is also true for the random graphs with multiple edges as defined in Sec. II B.) Above C_{crit} there are three contributions to $\langle \Omega \rangle$, from the three solutions. In total, there is a divergence at $C \rightarrow C_{\text{crit}}^+$. This results in the discontinuous function shown in Fig. 5(B). The finite- N curves that approach this asymptotic behavior are shown in Fig. 5(C), both from a numerical summation of Eq. (4) for finite N , and from exhaustive searches for FPs at small $N = 5, 15$.

Close to and above the transition, $\langle \Omega \rangle \sim \frac{1}{\sqrt{C-C_c}}$, see Appendix F. This can be derived from the general behavior of $q(\psi)$ near the transition, see Appendix F. The average number of FPs also depends in a different way on the number of sites: at $C = C_c$, $\langle \Omega \rangle \propto N^{\frac{1}{4}}$, whereas in the excitatory model, where the transition is second order, $\langle \Omega \rangle \propto N^{\frac{1}{3}}$.

In the excitatory model, we found that the transition is connected to the appearance of a subgraph that can be defined geometrically, the large strongly connected component. The vertices that belong to this can also be identified in a local way: by testing whether the outward and inward trees leaving the vertices grow exponentially for several generations or die off. In the double excitatory model, the sites that are on at a FP with $\psi = \psi^{(3)}$ also seem to have a geometrical interpretation, while those with $\psi = \psi^{(2)}$ seem not to, as suggested by the results of Ref. [28].

We have not calculated $\langle \Omega^2 \rangle$, but it will have the same qualitative features: For $C < C_{\text{crit}}$, there is exactly one FP; therefore $\langle \Omega^2 \rangle = 1$; above the transition $\langle \Omega^2 \rangle \geq \langle \Omega \rangle^2$ and so there will be a divergence.

D. The Inhibitory model

The inhibitory model is defined by: $x_i(t+1) = 1$ iff for all incoming edges $x_j(t) = 0$. It is of interest as a model of inhibitory interactions in neural networks, and ecological interactions between species. There is a phase transition in the magnetization dynamics at some value C_{crit} : $q(\psi)$ in the notation of Eq. (14) always has one fixed point ψ^* , but at C_{crit} it becomes unstable to a 2-cycle. The change in the dynamics does not lead to any singularity of $\langle \Omega \rangle$ since the fixed point becomes unstable via $q'(\psi^*)$ passing through -1 , so that Eq. (16) is finite. On the other hand, the second moment $\langle \Omega^2 \rangle$ diverges at C_{crit} , and at $C > C_{\text{crit}}$ there can be multiple clusters of FPs. The derivation is detailed in Appendix G.

The behavior of the moments is thus similar to the Kauffman model, although unlike in the Kauffman model the transition has an effect on the dynamics of the magnetization; this just does not lead to a singularity of $\langle \Omega \rangle$. The calculations are more complicated than in the Kauffman model, since the dynamics of two copies cannot be reduced to just the dynamics of the overlap fraction ϕ .

Simulations show that in this case, the fluctuating phase is not chaotic when parallel dynamics is used: specific configurations and not just the magnetization converge to 2-cycles⁷. (See also [29].) The behavior of $\langle \Omega \rangle$ and $\langle \Omega^2 \rangle$ is not influenced by these 2-cycles: all the contributions to moments come from the fixed values of ψ and $(\psi_{11}, \psi_{10}, \psi_{01}, \psi_{00})$ even though when $C > C_{\text{crit}}$ these are unstable fixed points and the dynamics does not visit them.

⁷ There can be finitely many sites that oscillate with a larger period

Finally, we note that $\langle \Omega \rangle$ has interesting behavior when $C \rightarrow \infty$ (after the limit $N \rightarrow \infty$): in graphs without self-loops, $\langle \Omega \rangle$ diverges at large C , while if self-loops are allowed, $\langle \Omega \rangle \rightarrow 0$ at large C . This qualitative effect on the behavior caused by removing self-loops is shown in Appendix G.

IV. DISCUSSION, OPEN QUESTIONS AND FUTURE DIRECTIONS

In this paper, we looked at the number and organization of fixed points in different sparsely-connected cellular automata, and how their properties are related to the dynamics. We have seen that at dynamical transitions the fixed points divide up into multiple clusters upon crossing the transition to the chaotic phase. The analysis shows a close connection between low moments and the dynamics; $\langle \Omega \rangle$ is related to the dynamics of the magnetization (see Eq. (16)) and $\langle \Omega^2 \rangle$ is related to the dynamics of the distance between two copies.

The examples we studied illustrate different universality classes of transitions. At each transition there is a certain change in the dynamics which leads to a certain type of singularity in $\langle \Omega \rangle$ or $\langle \Omega^2 \rangle$ as a function of $C - C_c$. The power laws can be understood by considering how the form of the graph $q(\psi)$ or $\tilde{q}(\vec{\phi})$ changes at the transition point (see Figs. 4 and 5). For example, for the double excitatory model, Sec. III C, $\langle \Omega \rangle \sim (C - C_c)^{-\gamma}$ at $C \rightarrow C_c^+$ with $\gamma = 1/2$. Similarly, the exponents $\gamma = 1$ on both sides of the transition in the excitatory model, the inhibitory model, and the Kauffman model can be justified. (This can also be used to calculate the ratio between the coefficient on the two sides of the transition.) These predictions apply to many systems and are independent of details such as the functions used, the vertex degrees, and whether there are loops or not.

In the frozen phase, the structure of the graphs and in particular the short loops, allows to reproduce the moments from a different perspective, and give even more information. In particular, they give the entire distribution $P(\Omega)$, (see Eq. (12) and Fig. 2) and show that for the Kauffman model, the probability of having a fixed point $P(\Omega > 0) \sim \sqrt{C_c - C}$. In the fluctuating phase, we can determine only moments of the number of fixed points, so we do not know how $P(\Omega > 0)$ changes as $C \rightarrow C_c^+$.

The work raises several interesting directions for future study. In the fluctuating phase, less is understood compared to the frozen phase, since we do not understand the structure of the fixed points in terms of changes in small subgraphs made of cycles and trees. We found that there are multiple clusters of similar FPs, such that FPs belonging to two different clusters involve extensive changes. What are the statistics of the number of clusters or of the number of fixed points in a cluster? Are there cases where the number of clusters diverges at the transition as well as the number of fixed points belonging to each cluster? Also, what is the probability of having no FPs near the transition (in analogy with the frozen phase)? We know only the moments of Ω in this phase, so we do not know whether $P(\Omega > 0) \sim \sqrt{|C_c - C|}$ also in this phase. Another interesting thing to consider is how the distributions of Ω differ between frozen and fluctuating phases. We have found that in many cases the moments of Ω behave in a similar way in both phases, although the algorithm for eliminating frozen sites leaves behind an extensive number of sites with overlapping loops. Also the dynamics is very different. In particular, in the fluctuating phases, contributions to the moments often come from unstable fixed points of q or \tilde{q} . Is the full distribution function, unlike the low moments, very different in the fluctuating phase?

Another direction regards higher moments. For example, are there models where the transition and associated singularities in the number of FPs are only found in $\langle \Omega^3 \rangle$ or higher moments?

Here we have discussed properties only of FPs. Of course, there remain very interesting but potentially very hard problems beyond FPs, such as the distribution of period lengths and basin sizes.

ACKNOWLEDGMENTS

We would like to thank Eric Brunet and Zhan Shi for discussions on the properties of the Lambert function and Paul D. Hanna for advice about the sum appearing in the inhibitory model.

Appendix A: Saddle points and mean field dynamics

The expressions for the expected number of fixed points can be interpreted in a conceptual way that helps understand their behavior at transitions for different models. We consider Boolean network models, with input sites chosen at random, such as the models discussed in this article.

For such models, there is a relationship between the function $q(\psi)$ that describes the time dependence of the magnetization, $\psi = \frac{N_1}{N}$, and the mean number of fixed points, see Eq. (15). The formulas for the models studied

here, the Kauffman model, double excitatory model, single excitatory model, and inhibitory model have this form, with different q 's. Notice that this formula is for the case where the edges coming into each site are chosen completely randomly and independently of one another; loops and double edges are not ruled out. Allowing loops changes the number of fixed points by a factor of order 1 (see the calculation for the inhibitory model for an example). The multiple edges can be shown to have no effect when N is large.

As explained in the main text, the sum is dominated by values in the vicinity of solutions to $\psi = q(\psi)$. Except when $\psi \approx 0$ or $\psi \approx 1$, the sum can be replaced by an integral. The Gaussian approximation to the binomial distribution gives the contribution near one of the fixed points ψ_i :

$$\int_{\psi_i - \epsilon N}^{\psi_i + \epsilon N} dN_1 \frac{1}{\sqrt{2\pi N q(1-q)}} e^{-\frac{(N_1 - q(\frac{N_1}{N}))^2}{2q(1-q)N}}, \quad (\text{A1})$$

where all factors of q stand for $q(\psi_i)$. (Except for the factor of $q(N_1/N)$ in the numerator, evaluating q at the saddle point ψ_i leads to a vanishing error.) Defining x by $N_1 = N\psi_i + x$, we find that $(N_1 - q(\frac{N_1}{N}))^2 \approx x^2(1 - q'(\psi_i))^2$. This makes the width of the Gaussian different by a factor of $\frac{1}{|1 - q'(\psi_i)|}$ without changing the height of it, so the integral is

$$\langle \Omega \rangle_{\psi_i} = \frac{1}{|1 - q'(\psi_i)|}. \quad (\text{A2})$$

The contributions to $\langle \Omega^k \rangle$ that can be described by integrals can be calculated the same way. This is the same as the *first* moment of the number of fixed points in k identical copies of the system. One can think of the replicas as being one system where each site has 2^k values. So to be more general, consider a system with l values and determine the first moment of $\langle \Omega \rangle$ for it; applying this to k replicas of a system gives the moments of the number of fixed points for it.

For a system with l values define a magnetization vector $\vec{\psi}$ with l components giving the fraction of sites with each of the l values. The dynamics of $\vec{\psi}$ is determined by a vector of l functions, $\vec{\psi}_{t+1} = \vec{q}(\vec{\psi}_t)$. The expected number of fixed points is given by a sum generalizing Eq.15, and the Gaussian approximation shows that near any $\vec{\psi}_i$ that is a fixed point of \vec{q} , whose components are nonzero, the expected number of fixed points [30] is

$$\left(\left| \det \mathbf{1} - \frac{(\partial \vec{q})'}{(\partial \vec{\psi})'} \right| \right)^{-1} \Bigg|_{\vec{\psi}_i} \quad (\text{A3})$$

where $\frac{(\partial \vec{q})'}{(\partial \vec{\psi})'}$ is the Jacobian matrix of $l-1$ components of $\vec{q}(\vec{\psi})$ as a function of the corresponding $l-1$ components of $\vec{\psi}$; since the variables $\vec{\psi}$ sum to 1, only $l-1$ of them are independent variables. (One can show that any $l-1$ components can be used). To evaluate a contribution to $\langle \Omega^2 \rangle$ this formula can be applied to the functions $q_{11}, q_{10}, q_{01}, q_{00}$ of $\psi_{11}, \psi_{10}, \psi_{01}, \psi_{00}$.

The Gaussian approximation to $\langle \Omega \rangle$ does not apply if $\psi_i = 0$ or 1 and the approximation to $\langle \Omega^2 \rangle$ does not apply if one of the components of $(\psi_{11}^{(i)}, \psi_{10}^{(i)}, \psi_{01}^{(i)}, \psi_{00}^{(i)})$ is zero, but the moments can still be written in terms of just the derivatives of q or \vec{q} at the extremum. For $\langle \Omega \rangle$, if the summand in Eq. (15) is written as $e^{NA(\psi)}$ and there is an extremum at an edge of the range of values for A , then the first derivative does not have to be zero. E.g., near $\psi = 0$ say $A(0) = 0, A'(0) < 0$, then $e^{NA(\psi)} \approx e^{-N|A'(0)|\psi} \approx e^{-|A'(0)|N_1}$. This decays exponentially over a scale of order 1, so the sum cannot be approximated by an integral.

If $\psi_i = 0$ satisfies $q(\psi) = \psi$ then for small N_1 's:

$$\binom{N}{N_1} q \left(\frac{N_1}{N} \right)^n \left(1 - q \left(\frac{N_1}{N} \right) \right)^{N-N_1} \approx \frac{N^{N_1}}{N_1!} \left(q'(0) \frac{N_1}{N} \right)^n \left(1 - q'(0) \frac{N_1}{N} \right)^{N-N_1} \approx \frac{[q'(0)e^{-q'(0)}]^{N_1} N_1^{N_1}}{N_1!},$$

which is more complicated than the exponential $e^{-|A'(0)|N_1}$ predicted at first (because A is not an analytic function near $N_1 = 0$) but is still independent of N and decays over a scale of order 1 as $N_1 \rightarrow \infty$. So by Eq. (B4),

$$\langle \Omega \rangle_{\psi \approx 0} \approx \sum_{N_1} \frac{e^{-q'(0)N_1} q'(0)^{N_1} N_1^{N_1}}{N_1!} = \frac{1}{1 + W(-q'(0)e^{-q'(0)})}. \quad (\text{A4})$$

Notice that when $q'(0) < 0$ this is equal to $\frac{1}{1 - q'(0)}$ by Eq. (B2)), which agrees with the result of the Gaussian approximation, although the sum is not Gaussian!

Similarly even near extrema where at least one of the components of $(\psi_{11}^{(i)}, \psi_{10}^{(i)}, \psi_{01}^{(i)}, \psi_{00}^{(i)})$ is zero, there are expressions for $\langle \Omega^2 \rangle$ that depend only on the derivatives of \vec{q} at the extremum. The sums cannot be summed immediately in terms of the Lambert function (they are sums over multiple variables). See Appendix C for the expressions.

Appendix B: Facts regarding the Lambert function

The Lambert W function[31], denoted by $W(x)$, is used several times throughout the text. It is defined as the solution to

$$W(x)e^{W(x)} = x. \quad (\text{B1})$$

For some x 's, this equation has two solutions; $W(x)$ is defined as the solution which is zero at $x = 0$ and whose value is in the range $-1 \leq W < \infty$, sometimes called W_0 . This function is real for $x \geq -1/e$.

Here are several useful relations that involve $W(x)$:

$$W(ye^y) = y \text{ if } y \geq -1 \quad (\text{B2})$$

The series expansion near 0 is

$$W(x) = x - x^2 + \frac{3x^3}{2} - \frac{8x^4}{3} + \dots = \sum_{n \geq 1} (-)^{n-1} x^n \frac{n^{n-1}}{n!},$$

see [32], Ch. 3, Sec. 10, pg. 114. This formula is connected to Cayley's formula for counting trees with n numbered vertices (see [33] pg. 48 and [34] chapter 4). The derivative satisfies:

$$\frac{1}{1+W(x)} + x \frac{dW(x)}{dx} = 1 \quad (\text{B3})$$

as can be seen by differentiating Eq. (B1). Substituting the series for $W(x)$ gives:

$$\frac{1}{1+W(x)} = \sum_{n \geq 0} (-)^n x^n \frac{n^n}{n!}. \quad (\text{B4})$$

Appendix C: Sum Expressions for $\langle \Omega^2 \rangle_{\text{near}}$

Consider the number of pairs of fixed points with a fraction of sites that are assigned state 1 equal to $\psi^{(i)}$. This corresponds to an extremum $(\psi_{11}, \psi_{10}, \psi_{01}, \psi_{00}) = (\psi^{(i)}, 0, 0, 1 - \psi^{(i)})$ in the sum for $\langle \Omega^2 \rangle$, with components that are zero, so the Gaussian approximation cannot be used. An expression that gives the number of pairs of FPs in terms of derivatives of \vec{q} nearby will now be derived. Such sums can also be derived for saddle points $\vec{\psi}^{(i)}$ where other combinations of components of $\vec{\psi}$ are 0. These saddle points occur in families of automata where there are FPs with two different fractions $\psi^{(1)}, \psi^{(2)}$. For example, if $\psi^{(1)} = 0$, then the correlation between the number of fixed points at $\psi \approx 0$ and at $\psi \approx \psi^{(2)}$ is described by a saddle point at $\vec{\psi} = (0, 0, \psi^{(2)}, 1 - \psi^{(2)})$. (This occurs in the excitatory model has this form, but it is easier to determine $\langle \Omega^2 \rangle$ from the distribution of Ω .)

We must evaluate the sum (7) near $(\psi^{(i)}, 0, 0, 1 - \psi^{(i)})$. Since $N_{11} + N_{10} + N_{01} + N_{00} = 1$, let us take N_{11}, N_{10}, N_{01} as independent variables. The sum will be over finite values of N_{10}, N_{01} and N_{11}/N close to $\psi^{(i)}$. Let us define $k = N_{10}, l = N_{01}, n = N_{11}, \bar{\theta} = n/N$, and

$$t_{n,k,l} = \binom{N}{k, l, n, N-k-l-n} q_{10}^k q_{01}^l q_{11}^n q_{00}^{N-n-k-l}.$$

Consider the effects of k, l on the values of $q_{10} = q_{10}(\frac{n}{N}, \frac{k}{N}, \frac{l}{N})$, etc. If two configurations are the same aside from a small number of sites then applying the automaton to them will give two configurations that are also close to each

other, so $q_{10}(\frac{n}{N}, 0, 0) = 0$. Also $q_{11}(\frac{n}{N}, 0, 0) = q(\frac{n}{N})$ because when the configurations are identical, they evolve by the dynamics of a single configuration. The result of expanding $q_{10}(\frac{n}{N}, \frac{k}{N}, \frac{l}{N})$ to first order in $\frac{k}{N}, \frac{l}{N}$ is

$$\begin{aligned} q_{10} &= \frac{1}{N}a(k, l, \bar{\theta}) := \frac{k}{N} \frac{\partial q_{10}}{\partial \psi_{10}}(\bar{\theta}, 0, 0) + \frac{l}{N} \frac{\partial q_{10}}{\partial \psi_{01}}(\bar{\theta}, 0, 0) \\ q_{01} &= \frac{1}{N}b(k, l, \bar{\theta}) := \frac{k}{N} \frac{\partial q_{01}}{\partial \psi_{10}}(\bar{\theta}, 0, 0) + \frac{l}{N} \frac{\partial q_{01}}{\partial \psi_{01}}(\bar{\theta}, 0, 0) \\ q_{11} &= q(\bar{\theta}) + \frac{1}{N}c(k, l, \bar{\theta}) \\ q_{00} &= 1 - q(\bar{\theta}) + \frac{1}{N}d(k, l, \bar{\theta}) \end{aligned} \quad (C1)$$

where c, d are not written out since they will not matter, aside from satisfying the condition $a + b + c + d = 0$ because the total sum of q_{ij} is 1.

The term $t_{n,k,l}$ can be simplified by factoring it: $\binom{N}{n,k,l,N-n-k-l} \left(\frac{a}{N}\right)^k \left(\frac{b}{N}\right)^l q_{11}^n q_{00}^{N-n-k-l} = \binom{N}{k,l,N-k-l} \left(\frac{a}{N}\right)^k \left(\frac{b}{N}\right)^l \times \binom{N-k-l}{n,N-n-k-l} q_{11}^n q_{00}^{N-n-k-l}$. The first factor is approximately $\frac{a^k b^l}{k!l!}$. To approximate the second factor assume that $n = Nq_{11} + x\sqrt{N}$ so that $N - n - k - l = N(1 - q_{11}) - x\sqrt{N} = Nq_{00} + a + b - k - l - x\sqrt{N}$, and then use Stirling's formula to approximate the binomial coefficient. This gives $\frac{1}{\sqrt{2\pi Nq_{11}(1-q_{11})}} e^{-a-b-\frac{x^2}{2q_{11}(1-q_{11})}}$. This is a Gaussian distribution, aside from e^{-a-b} . This combines with the first factor to give $\frac{a^k b^l}{k!l!} e^{-a-b}$, showing that k and l have a Poisson distribution⁸. So

$$t_{n,k,l} \approx \left[\frac{e^{-a-b} a^k b^l}{k!l!} \right] \left[\frac{1}{\sqrt{2\pi Nq_{11}(1-q_{11})}} e^{-\frac{N(\bar{\theta}-q(\bar{\theta}))^2}{2q_{11}(1-q_{11})}} \right],$$

where the approximation $x = \frac{1}{\sqrt{N}}(n - Nq_{11}(n/N, k/N, l/N)) \approx \frac{1}{\sqrt{N}}(n - Nq(n/N))$ has been made. This result can be derived conceptually by saying that the probability that specific k sites have the value 10 and specific l sites have the value 01 is $\left(\frac{a}{N}\right)^k \left(\frac{b}{N}\right)^l$, the chance that no other sites have these values is $(1 - \frac{a+b}{N})^{N-k-l} \approx e^{-a-b}$, the number of possibilities for these $k+l$ sites is $\binom{N}{k,l,N-k-l} \approx \frac{N^{k+l}}{k!l!}$. These factors multiply to give the Poisson distribution. The e^{-a-b} comes from $q_{11}^n q_{00}^{N-n-k-l}$ because this describes the probability that certain sites are 11 or 00, Among the remaining sites the number of sites assigned 11, N_{11} has a Gaussian distribution with a mean of $q_{11}(N - k - l)$, but the shift by $k+l$ can be neglected.

When this is summed over k, l, n , the values of n where the second factor is large are near solutions to $q(\bar{\theta}) = \bar{\theta}$, e.g., near $\psi^{(i)}$. The first factor is smooth as a function of $\bar{\theta}$ since k and l are of order 1, so $\bar{\theta}$ can be replaced by $\psi^{(i)}$ in a and b . Eq. (C1) implies $a = \kappa_1 k + \kappa_2 l$, $b = \kappa_2 k + \kappa_1 l$, where $\kappa_1 = \frac{\partial q_{10}}{\partial \psi_{10}}(\psi^{(i)}, 0, 0)$, $\kappa_2 = \frac{\partial q_{10}}{\partial \psi_{01}}(\psi^{(i)}, 0, 0)$. So

$$\begin{aligned} \langle \Omega^2 \rangle_{\text{near}, \psi^{(i)}} &= \langle \Omega \rangle \sum_{k=0}^{\infty} \sum_{l=0}^{\infty} \frac{(k\kappa_1 + l\kappa_2)^k}{k!} \frac{(k\kappa_2 + l\kappa_1)^l}{l!} e^{-(\kappa_1 + \kappa_2)(k+l)}, \\ &= \frac{1}{|1 - q'(\psi^{(i)})|} \sum_{k=0}^{\infty} \sum_{l=0}^{\infty} \frac{(k\kappa_1 + l\kappa_2)^k}{k!} \frac{(k\kappa_2 + l\kappa_1)^l}{l!} e^{-(\kappa_1 + \kappa_2)(k+l)} \end{aligned} \quad (C2)$$

where we have noticed that the sum over n gives $\langle \Omega \rangle$, as in Eq. (A1), which involves only the derivatives of the q functions at $(\psi^{(i)}, 0, 0, 1 - \psi^{(i)})$.

Appendix D: Determined Sites in the Kauffman Model

Sec. IIC described a method of searching for fixed points of a Kauffman network. The algorithm finds certain sites whose values are determined at a fixed point. If there are only a small number of sites left over after this algorithm,

⁸ To give this an intuitive interpretation, consider $\binom{N}{n',k',l',N-n'-k'-l'} q_{10}(n, k, l)^k q_{01}(n, k, l)^l q_{11}(n, k, l)^n q_{00}(n, k, l)^{N-n'-k'-l'}$, which is the probability that if a configuration has $n, k, l, N - n - k - l$ sites assigned 11, 10, 01, 00 respectively, that after one step of evolution it will have $n', k', l', N - n' - k' - l'$ sites with these values. The second moment is the sum over this after letting $n = n', k = k', l = l'$. If k and l are small, k' and l' have a Poisson distribution because each site has only a small chance of being connected to a site in the state 10 or 01 and being caused to change to 10 or 01, and these sites are independent of one another.

then it allows one to find all the fixed points (not missing fixed points with a small basin of attraction for example) by searching through the combinations of possible values for the remaining sites. This works in the frozen phase of the Kauffman model. We here give an argument for why the fraction of sites remaining after the action of the algorithm is zero when $N \gg 1$.

To see why this happens, we will give an argument similar to [25], see also [18, 19]. The algorithm for finding which points are determined can be thought of as a system with three values, 0, 1, u (standing for “unknown”). We will not erase the arrows or the sites as in the version of the algorithm described above. We start initially with all sites in the state u . Then when rule (1) determines the value of a site, u is replaced by this value. This happens when each input site is definite or does not affect the function for the site. Once a site is assigned 0 or 1, its value will never change.

If the number of unknown inputs to a site is k , the chance that it will be known at the next step is $2 / \binom{2^k}{2}$; 2^{2^k} is the number of functions of the unknown variables, and 2 is the number of these that do not depend on the input. If ψ_u is the fraction of unknown sites at a step, then the fraction of unknown sites at the next step is:

$$q_u(\psi_u) = \sum_{k=0}^{\infty} \left(1 - \frac{2}{2^{2^k}}\right) e^{-C\psi_u} \frac{(C\psi_u)^k}{k!}.$$

This always has a fixed point at $\psi_u = 0$, and it is attractive when $C < 2$ because $q'_u(0) = C/2$. This function does not seem to have any other fixed points when $C < 2$, so as the process is iterated $\psi_u \rightarrow 0$, thus only a sub-extensive number of sites is undetermined.

This algorithm gives a way to find the fixed points of the Kauffman model in the frozen phase, but it seems likely that there can be frozen phases of other models whose fixed points cannot be found this way. For example, in a model where none of the input functions are constant functions, there are no sites whose values are known for sure at the beginning, yet some of these models seem likely to allow for frozen phases. A simple example where no site’s value is immediately determined, but there is still a unique fixed point, is a sequence of $2n$ sites with values 0, 1 where the functions are $x_i(t+1) = x_{i-1}(t)$ for $2 \leq i \leq 2n$ and $x_1(t+1) = x_n(t) + x_{2n}(t) - 2x_n(t)x_{2n}(t)$. (Every site’s value depends on other sites’ values, so there is no site that is immediately determined. But one can see that nevertheless, there is only one fixed point, where all sites are 0.)

A random network that seems also to have the behavior where the values of sites at fixed points are determined although there is no way to determine these values by backtracking for a small number of steps, is one where all sites have two inputs and the functions are either $x_i(t+1) = x_{j_1}(t)x_{j_2}(t)$ (with probability p) or $x_i(t+1) = 1 - x_{j_1}(t)x_{j_2}(t)$ (with probability $1 - p$). For $1 > p > p_c$, one finds that there is only one saddle point in the sum representing $\langle \Omega^2 \rangle$ and it has $\psi_{01} = \psi_{10} = 0$, so that there is only one cluster of fixed points.

Appendix E: Derivation details for the excitatory model

The excitatory model’s behavior is determined entirely by topological properties of random directed graphs, which have a transition similar to the Erdős–Rényi transition in undirected graphs where a large connected component forms at a critical connectivity, see [35] Chapter 10. (In this section we will assume the random graphs are directed Erdős–Rényi graphs, with loops allowed, rather than the graphs with multiple edges used elsewhere in the paper. As stated above, this does not affect the moments of $\langle \Omega \rangle$ when N is large. This is checked in footnote 9.) The number of fixed points is the number of ways to assign 0 and 1’s to the sites of the directed graph so that if s is the value at a site and s_1, s_2, \dots, s_p are the values at sites directed toward it, then $s = \max\{s_1, s_2, \dots, s_p\}$ —it is the maximum of all its inputs. We note that loops provide the flexibility that allows for multiple fixed points: On a tree, all sites must have value 0, since, arguing by contradiction, if a site has value 1 there must be an upstream path with all values 1, but any path in a tree must end at a site with no inputs. On the other hand, a loop in isolation can be assigned either all zeros or all ones, and the same applies for an isolated SCC.

Consider a general directed graph. Not all sites belong to SCCs, since a vertex might not belong to any directed loop. One can see that the values for sites that do not belong to SCCs are determined by the SCCs that are upstream from them—they must be assigned zero if all SCCs with paths leading to them have the value 0 (or if there are no SCCs leading to them) and otherwise they are assigned the value 1. Thus, values need only be chosen for the SCCs.

Now the values assigned to the SCCs have conditions on them. Consider the reduced graph where each SCC is represented by a vertex, and there is a directed edge between two such vertices if there is a directed path connecting them. This graph does not have directed cycles in it since all the SCCs on a cycle would in fact be a single SCC. On this graph, if s is the value assigned to an SCC and s_1, s_2, \dots, s_p are the values of the SCCs directed toward it, then $s \geq \max\{s_1, s_2, \dots, s_p\}$. Note that this is different from the constraint on the original graph because of the inequality

sign: an SCC can have the value 1 even if all inputs are 0 because the cycles within itself allow this. The number of fixed points is the number of ways to assign the values to the SCCs, following this constraint.

The graph obtained by reducing a graph to the graph of its SCCs may have a complex structure, but for an Erdős–Rényi graph, it has a simple structure with probability one, and this makes it easy to determine all the solutions to the above constraint. We first note the difference between directed and undirected Erdős–Rényi graphs. For undirected random graphs, when the number of edges is greater than the critical number, there is a giant component which contains a finite fraction of all vertices, while the other vertices belong to components whose sizes are all small. In the directed graph, there are different degrees of connectivity. Thus, besides the giant SCC and vertices that are not connected to it by directed paths, there are two other sets of vertices: vertices which have paths *leading to* the giant SCC and vertices with paths arriving at them *from* it. Each of these sets of sites is extensive. But the vertices that are important for counting fixed points are the ones belonging to SCCs, and besides the giant SCC, there are a finite number of these, each containing one loop. They may be upstream, downstream, or disconnected from the giant SCC, but there are no directed paths directly between the small SCCs. The reason is that the chance of two small subgraphs being connected by a *short* path is $\sim 1/N$ since the chance of connections between specific vertices is $\sim 1/N$. On the other hand, if they are connected by a *long* path it is likely that some of the vertices on it belong to the giant SCC. Thus the structure of the graph of SCCs is as indicated in Fig. 4(D).

This allows us to count the number of fixed points in the case $C < 1$ and $C > 1$, where 1 is the point where the giant SCC appears. If $C < 1$, there are $O(1)$ SCCs, each with one cycle in it and no directed paths between them, so each one can be assigned 0 or 1 independently. Thus if there are k SCCs, there are 2^k fixed points. When there is a giant component, each cycle is constrained by the cycles that are upstream from it. If there are k_{up} , k_{down} , and k_{disc} SCCs that are upstream, downstream and disconnected from the giant SCC, then the SCCs can be counted as follows. If the value of the giant component is 1, then the downstream components must have the value 1, while if the giant component has value 0, the components upstream from it must have the value zero. The rest of the components can have arbitrary values. Thus the number of fixed points in the two cases is $2^{k_{up}+k_{disc}}$ and $2^{k_{down}+k_{disc}}$ respectively or $2^{k_{disc}}(2^{k_{up}} + 2^{k_{down}})$ fixed points altogether.

To understand the size of the giant component, consider any site of the network. If one follows edges out from this, they form a tree locally. The number of outgoing edges from each vertex in this tree has a Poisson distribution with mean C . Thus, when $C < 1$, the mean number of descendants decreases exponentially with the generation, so the tree ends. There can be no giant component then. If $C > 1$, then if the tree does not die out after a small number of steps, it will keep growing and then it must contain points in the SCC. Let Q be the chance that a tree starting from a given site dies out so that the site does not connect to the giant component. This may be related to itself: for the vertex to not have a path toward the giant component means that each site adjacent to it does not have paths to the giant component. That is:

$$Q = \sum_{j=0}^{\infty} P(j \text{ descendants}) Q^j = \sum_{j=0}^{\infty} \frac{e^{-C} (CQ)^j}{j!} = e^{C(Q-1)}$$

The solution is $Q = -W(-Ce^{-c})/C$. The probability to *belong* to the giant component is the probability that both the outgoing and incoming trees from the site do percolate, $(1 - Q)^2$. Thus the giant SCC has $(1 - Q)^2 N$ sites on average. Next, consider the number of sites that have the same value as the giant component at the fixed points, i.e. the sites downstream from it. These have connections to the giant component in one direction but not the other, so there are $Q(1 - Q)N$ of them.

Next apply this reasoning to find the number of short cycles, and hence the number of fixed points:

Below the percolation transition, $C < 1$: The number of fixed points is given by $\Omega = 2^k$ where k is the number of SCCs. The number of cycles of length n is Poisson distributed with mean $\lambda_n = C^n/n$. Therefore, the mean of the total number of cycles is

$$\lambda = \sum_{n=1}^{\infty} \lambda_n = \ln \frac{1}{1 - C},$$

and the distribution of the total number is a Poisson distribution also. So the probability distribution for the number of fixed points is:

$$P(n \text{ FP}) = \begin{cases} [1 - C] \frac{(\ln(\frac{1}{1-C}))^k}{k!} & n = 2^k \\ 0 & \text{else} \end{cases}$$

The moments are:

$$\langle \Omega^r \rangle = \sum_{k=0}^{\infty} 2^{kr} P(2^k \text{ FP}) = \left(\frac{1}{1 - C} \right)^{2^r - 1}. \quad (\text{E1})$$

This diverges at $C = 1$ with exponent $2^r - 1$.

Above the percolation transition, $C > 1$: The number of fixed points depends on k_{up} , k_{down} , and k_{discon} as discussed above. To understand their statistics, note that a short cycle will be in an SCC upstream from the giant component if at least one of its sites has a macroscopic tree leaving it, and none have a macroscopic tree going into it. (In the latter case it would be part of the giant component). The sites that are upstream and downstream from the SCC are not correlated, so this probability is $Q^n(1 - Q^n)$ where n is the number of sites in the cycle. As different cycles are uncorrelated, k_{up} is a Poisson variable with the mean $\lambda_{\text{up}} = \sum_{n=1}^{\infty} \frac{C^n}{n} Q^n(1 - Q^n) = \log \frac{1-CQ^2}{1-CQ}$; similarly for k_{down} . A cycle is unconnected to the giant component with probability Q^{2j} , so k_{disc} is a Poisson variable whose mean is $\lambda_{\text{discon}} = \log \frac{1}{1-CQ^2}$.

Thus,

$$\langle \Omega \rangle = \langle 2^{r_{\text{discon}}} (2^{r_{\text{up}} + r_{\text{down}}}) \rangle = 2e^{\lambda_{\text{up}} + \lambda_{\text{discon}}} = \frac{2}{1-CQ} = \frac{2}{1+W(-Ce^{-C})}. \quad (\text{E2})$$

The fixed points just found belong to two clusters: all the FPs where the giant component has the value 1 are a finite distance from one another, since only the values on short cycles upstream from the SCC vary; likewise all the FPs where the giant component has the value 0 are a finite distance from one another. For the latter case, $\psi = 0$, while for the former, $\psi = (1 - Q)^2 + Q(1 - Q) = 1 - Q$ since both the sites in the giant component and downstream from it have the value 1; these agree with the two fixed points of $\psi \rightarrow q(\psi)$.

Near and above the transition, where $C = 1 + \varepsilon$, one can show that $Q = 1 - 2\varepsilon + O(\varepsilon^2)$. Then $\langle \Omega \rangle \sim \frac{2}{C-1}$. Below the transition the divergence is $\langle \Omega \rangle \sim \frac{1}{1-C}$.

Now we will calculate the expected number of fixed points using Eq. (15), to compare with the above results. Recall that we are not allowing double edges in this section (as mentioned in Sec. II B this does not affect the answer). That is, each directed edge (including loops) is added to the graph with a probability of $\frac{C}{N}$. We have

$$\langle \Omega \rangle = \sum_{N_1=0}^N \binom{N}{N_1} \left[\left(1 - \frac{C}{N}\right)^{N_1} \right]^{N-N_1} \left[1 - \left(1 - \frac{C}{N}\right)^{N_1} \right]^{N_1}. \quad (\text{E3})$$

which has the form of Eq. (15) with $q(\psi) \approx 1 - e^{-C\psi}$ where $\psi = \frac{N_1}{N}$. Note that $q(\psi) = 1 - e^{-C\psi}$ is the form that q takes when multiple edges are allowed; thus multiple edges do not affect $\langle \Omega \rangle^9$. The maxima in this sum are the solutions to $\psi = q(\psi)$. One solution is always $\psi_1^* = 0$ while if $C > 1$ there is a second solution. If $C > 1$, the former corresponds to the FPs where the giant component and the sites upstream from it are assigned 0, while the latter corresponds to the FPs where the giant component and the sites downstream from it are assigned 1. The contribution to $\langle \Omega \rangle$ from $\psi \approx 0$ is

$$\langle \Omega \rangle_{\psi \approx 0} \approx \sum_{N_1=0}^{\infty} \frac{N^{N_1}}{N_1!} e^{-CN_1} \left(\frac{N_1 C}{N} \right)^{N_1} \approx \sum_{N_1=0}^{\infty} (Ce^{-c})^{N_1} \frac{N_1^{N_1}}{N_1!} \quad (\text{E4})$$

By equation (B4) this is equal to $\frac{1}{1+W(-Ce^{-c})}$. This gives

$$\langle \Omega \rangle_{\psi \approx 0} = \begin{cases} \frac{1}{1-C} & \text{if } C < 1 \\ \frac{1}{1+W(-Ce^{-c})} & \text{if } C > 1, \end{cases}$$

which used Eq. (B2) when $C < 1$. This agrees with Eq. E1 when $C < 1$ and half of Eq. E2 when $C > 1$.

The other half of the fixed points in Eq. (6) should come from the other extremum. This extremum is the nonzero solution to $\psi = q(\psi)$, $\psi_2^* = 1 + W(-Ce^{-C})/C$. Note that this agrees with the magnetization $1 - Q$ of FPs with the giant component having the value 1. The number of fixed points is expected to equal $\langle \Omega \rangle_{\psi \approx 0}$ based on the symmetry between upstream and downstream components, although the symmetry is not obvious from Eq. (E3): the sum near $\psi_2^* = 1 - Q$ has a Gaussian form in contrast to the sum giving $\langle \Omega \rangle_{\psi \approx 0}$. However, using Eq.(A2) shows that it is also equal to $\langle \Omega \rangle_{\psi \approx 1-Q} = \frac{1}{1-Ce^{-C\psi}} = \frac{1}{1+W(-Ce^{-c})}$.

⁹ Replacing $q = 1 - (1 - \frac{C}{N})^{N_1}$ by $1 - e^{-C\psi}$ at first seems to produce an error of order 1: the error $(1 - \frac{C}{N})^{N_1} - e^{-C\psi}$ is of order $\frac{1}{N}$ (if N_1 is extensive). Since q is raised to a power of order N in Eq. (E3), it seems that this discrepancy will change the result by a factor of order 1. But the sum can be evaluated using Eq. A2, which does not involve raising q to a large power, so the error in the sum is negligible. The way both the exact sum and the approximate sum come out the same is that their terms, graphed as a function of ψ , are shifted by a small amount from one another. Since the peak is narrow, this makes an order 1 difference to the terms, but the total sums are equal.

Appendix F: Derivation details for the double-excitatory model

1. Dynamics

Let ψ_n be the mean magnetization (fraction of variables with $x_i = 1$) at time n . The dynamical update rule reads

$$\psi_{t+1} = \sum_{k=0}^{\infty} P_k \left[1 - (1 - \psi_t)^k - k\psi_t (1 - \psi_t)^{k-1} \right],$$

where P_k is the probability for k incoming edges. For a Poisson distribution, $P_k = e^{-C} C^k / k!$, so

$$\psi_{t+1} = q(\psi_t) = 1 - e^{-C\psi_t} (C\psi_t + 1)$$

This always has a fixed-point solution. For $C < C_{\text{crit}} \simeq 3.35$, the $\psi = 0$ solution is unique. For $C > C_{\text{crit}}$, there are three solutions and the middle one is unstable, so the dynamics reach either the smallest or largest fixed ones, depending on the initial conditions. See Fig. 5(A).

2. Counting FPs

The first moment, $\langle \Omega \rangle$, is given by

$$\begin{aligned} \langle \Omega \rangle &= \sum_{N_1=0}^{\infty} \binom{N}{N_1} \left[(1 - C/N)^{N_1} + N_1 \frac{C}{N} (1 - C/N)^{N_1-1} \right]^{N-N_1} \left[1 - (1 - C/N)^{N_1} - N_1 (1 - C/N)^{N_1-1} \frac{C}{N} \right]^{N_1} \\ &\equiv \sum_{N_1=0}^{\infty} \Omega_{N_1} \end{aligned}$$

The first two terms are to be interpreted as $\Omega_{N^*=0} = 1$ and $\Omega_{N^*=1} = 0$. As in the last section, this formula assumes multiple edges are not allowed, although this does not change the results for $N \gg 1$.

We now consider the saddle point approximation to this. At $C < C_{\text{crit}}$ the only contribution is at $\psi_1^* = N_1/N = 0$. One can check that only the $N_1 = 0$ term survives when $N \rightarrow \infty$, for which $\Omega_{N_1=0} = 1$. (Even terms where N_1 remains finite tend to zero.) At $C > C_{\text{crit}}$, there are 3 contributions, at the fixed points $\psi_{n+1} = \psi_n$ of the dynamical equation above. The saddle-point around each of the two maxima at $\psi > 0$ gives (by Eq. A2)

$$\frac{C\psi + 1}{|(\psi - 1)\psi C^2 + \psi C + 1|}$$

so the result at $C > C_{\text{crit}}$ is

$$\langle \Omega \rangle = 1 + \sum_{i=2,3} \frac{C\psi_i^* + 1}{|C^2\psi_i^*(\psi_i^* - 1) + C\psi_i^* + 1|}$$

where $\psi_{2,3}^*$ are the two nonzero fixed points solutions. This diverges at the transition, $C \rightarrow C_{\text{crit}}^+$. Overall there is a divergence only from one side of the transition, see Fig. 5.. Also, the power law is $\langle \Omega \rangle \propto \frac{1}{(C - C_{\text{crit}})^{1/2}}$ in contrast to the single excitatory model.

The $\langle \Omega \rangle \propto \frac{1}{(C - C_{\text{crit}})^{1/2}}$ divergence can be derived from the general behavior of $q(\psi)$ near the transition. The graph of $q(\psi)$ first touches the line $y = x$ at C_c . Say the point where they touch is ψ_0 . This implies that when $C = C_c + \epsilon$, $q(\psi) - \psi_0 = a(\epsilon) + b(\epsilon)(\psi - \psi_0) - c(\psi - \psi_0)^2$, with $a(\epsilon) = a'_0\epsilon$ and $b(\epsilon) = 1 + b'_0\epsilon$. The fixed points are at $(b'_0\epsilon \pm \sqrt{4a'_0c\epsilon}) / (2c)$ and the value of $\frac{dq}{d\psi}$ at them is $1 \mp \sqrt{4a'_0c\epsilon}$, so $\langle \Omega \rangle = \frac{2}{\sqrt{4a'_0c\epsilon}}$.

Without working out $\langle \Omega^2 \rangle$, it must have qualitatively the same behavior. For $C < C_{\text{crit}}$, there is exactly one FP, therefore $\langle \Omega^2 \rangle = 1$, and above the transition $\langle \Omega^2 \rangle \geq \langle \Omega \rangle^2$ and so there will be a divergence. Whether C is bigger or smaller than C_{crit} , there is always a unique fixed point near $\psi_1^* = 0$, the one where all sites are off. As in Sec. II C, any other fixed point nearby would differ from this at cycles with trees going out from them. But then the sites of

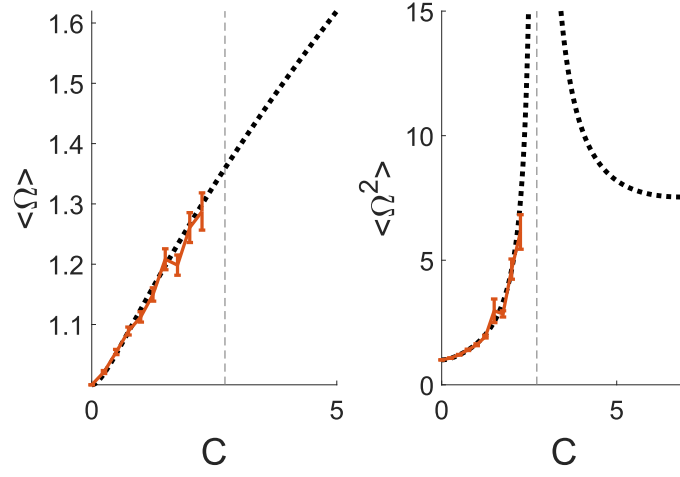


Figure 6. Analytical results for $\langle \Omega \rangle$ and $\langle \Omega^2 \rangle$ (dashed lines) for the inhibitory model, compared to exhaustive numerical searches (error bars) at $N = 5000$.

the graph do not satisfy the condition of having inputs from at least two other sites that are on, since all sites outside the subgraph are off. But there can be pairs of FPs that are close to each other when $\psi > 0$. We have the following example: for a cycle with exactly one incoming edge from an active site (from outside the cycle) to each vertex, the entire cycle can be either on or off. As long as this does not affect many sites downstream, this gives two nearby stationary configurations.

Appendix G: Derivation details for the inhibitory model

In this Appendix we present the calculation of $\langle \Omega \rangle$ and $\langle \Omega^2 \rangle$ for the inhibitory model, as well as $P(\Omega)$ in the frozen phase. The results for $\langle \Omega \rangle$ and $\langle \Omega^2 \rangle$ are plotted in Fig. 6, and compared to an exhaustive search algorithm in the frozen phase ($C < e$ in this model).

As for the Kauffman model, in the frozen phase we find that a graph simplification algorithm allows to simplify large graphs with thousands of sites, until exhaustive search for FPs is possible. It repeats the following steps, that do not change the number of FPs, until no further changes are possible:

1. Remove all sites i that have no incoming edges, and all outgoing edges from these sites (including the vertices that they point toward). This can be done because a site i with no inputs will have $x_i = 1$ at all FPs, and if site i is an input to site j then at all FPs $x_j = 0$, so site j does not affect any other site.
2. Remove all sites that have no outgoing edges.

1. 1st moment

Consider a configuration with N_1 sites that are on and $N - N_1$ that are off, and determine the probability that it will be a fixed point when the connections are assigned. A site that is on will stay on if all inputs are off. The probability is $(1 - \frac{N_1}{N})^k$ when there are k inputs. Hence

$$q(\psi) = \sum_{k=0}^{\infty} e^{-C} \frac{C^k}{k!} \left(1 - \frac{N_1}{N}\right)^k = e^{-C\psi}. \quad (\text{G1})$$

(This assumes the graph is constructed as in Sec.II B, with multiple edges allowed).

Thus the average number of fixed points is as in Eq. (15),

$$\langle \Omega \rangle = \sum_{N_1=0}^N \binom{N}{N_1} q \left(\frac{N_1}{N}\right)^{N_1} \left(1 - q \left(\frac{N_1}{N}\right)\right)^{N-N_1} \equiv \sum_{N_1=0}^N \Omega_{N_1}. \quad (\text{G2})$$

The contribution to the saddle point approximation is at the solution to $q(\psi) = \psi$ (see Sec. III), namely $\psi^*(C) = \frac{W(C)}{C}$ where W is the Lambert W function, which gives (according to Eq. (A2))

$$\langle \Omega \rangle = \frac{1}{1 + W(C)}$$

This is an analytic function of C with no singularities.

2. 2nd moment

Take two configurations, with $N_{00}, N_{10}, N_{01}, N_{11}$ the numbers of sites with the pairs of values 00, 10, 01, 11. Also let $\psi_{00} = \frac{N_{00}}{N}$ etc. The probability that this is a fixed point is $q_{00}^{N_{00}} q_{01}^{N_{01}} q_{10}^{N_{10}} q_{11}^{N_{11}}$ where q_{00} is the probability that the inputs to a site would cause it to become 00 at the next step, etc. Then

$$q_{11} = \sum_{k=0}^{\infty} e^{-C} \frac{C^k}{k!} \psi_{00}^k = e^{-C(1-\psi_{00})} \quad (\text{G3})$$

where the sum is over the number of incoming edges. Also,

$$q_{10} = \sum_k e^{-C} \frac{C^k}{k!} [(\psi_{01} + \psi_{00})^k - \psi_{00}^k] = e^{-C(1-\psi_{00})} [e^{C\psi_{01}} - 1]. \quad (\text{G4})$$

while the formula for q_{01} is similar and $q_{00} = 1 - q_{11} - q_{01} - q_{10}$. The 2nd moment is given by Eq. (7).

$$\langle \Omega^2 \rangle = \sum_{N_{11}, N_{01}, N_{10}} \binom{N}{N_{00}, N_{01}, N_{10}, N_{01}} q_{11}^{N_{11}} q_{00}^{N_{00}} q_{01}^{N_{01}} q_{10}^{N_{10}} \equiv \sum_{N_{11}, N_{01}, N_{10}} \Omega_{N_{11}, N_{01}, N_{10}} \quad (\text{G5})$$

The extrema are at solutions to $\vec{\psi} = \vec{q}(\vec{\psi})$. This condition always has a solution corresponding to two fixed points in the same cluster, $\psi_{01} = \psi_{10} = 0$, $\psi_{11} = \frac{W(C)}{C}$, and when $C > C_{\text{crit}} = e$ another solution given by

$$\begin{aligned} \psi_{11} &= -\frac{W\left(-\frac{W^2(C)}{C}\right)}{C} \\ \psi_{01} = \psi_{10} &= \frac{W(C)}{C} + \frac{W\left(-\frac{W^2(C)}{C}\right)}{C}. \end{aligned} \quad (\text{G6})$$

(Notice that these equations are consistent with the fixed point that occurs in one copy of the system: $\psi_{11} + \psi_{10} = \psi$ because this counts the number of sites in the first copy with the value 1.) This represents a pair of fixed points not in the same cluster. For large C , $\psi_{11} \ll \psi_{01}, \psi_{10}$, so there is little overlap between FPs except for ones that are essentially identical. In fact, ψ (the fraction of sites equal to 1 in a typical fixed point) is approximately $\frac{\log C}{C}$ and $\psi_{11} \approx \left(\frac{\log C}{C}\right)^2$ so it is as if different fixed points are made up of independently chosen sets.

Eq. G5 can be summed using the saddle point approximations given above. The contribution from the first fixed point, $\psi_{10} = \psi_{01} = 0, \psi_{11} = \frac{W(C)}{C}$ can be evaluated using Eq. C2, $\langle \Omega^2 \rangle = \langle \Omega \rangle \sum_{k_1, k_2} \frac{k_1^{k_2} k_2^{k_1}}{k_1! k_2!} \left(\frac{W(C)}{C}\right)^{k_1 + k_2}$. We see numerically that the series is equal to

$$\sum_{k_1, k_2} \frac{k_1^{k_2} k_2^{k_1}}{k_1! k_2!} y^{k_1 + k_2} = \frac{1}{1 - W^2(-y)} = \frac{1}{1 - W^2\left(-\frac{W(C)}{C}\right)} \quad (\text{G7})$$

This expression can be proved using interesting identities about binomial coefficients (see Appendix H). Below the transition, for $C < e$, this is the only saddle-point contribution to the sum. Here, one can show¹⁰ that $W(C) =$

¹⁰ Using $W(C)e^{W(C)} = C$, it follows that $-\frac{W(C)^2}{C} = -W(C)e^{-W(C)}$. So if $x = W\left(-\frac{W(C)^2}{C}\right)$ then $xe^x = -W(C)e^{-W(C)}$. A solution is $x = -W(C)$, which can be checked to be the correct branch when $C < e$.

$-W\left(-\frac{W^2(C)}{C}\right)$, so

$$\langle\Omega^2\rangle = \langle\Omega^2\rangle_{\text{near}} = \langle\Omega\rangle \frac{1}{1-W^2(C)} = \frac{1}{(1+W(C))^2(1-W(C))} \text{ for } C < C_{\text{crit}}.$$

Above C_{crit} , there is also the second contribution, from near Eq. G6, which can be evaluated using Eq. A3:

$$(\langle\Omega^2\rangle_{\text{far}})^{-1} = \begin{vmatrix} 1 - \frac{\partial q_{11}}{\partial \psi_{11}} & -\frac{\partial q_{11}}{\partial \psi_{10}} & -\frac{\partial q_{11}}{\partial \psi_{01}} \\ -\frac{\partial q_{10}}{\partial \psi_{11}} & 1 - \frac{\partial q_{10}}{\partial \psi_{10}} & -\frac{\partial q_{10}}{\partial \psi_{01}} \\ -\frac{\partial q_{01}}{\partial \psi_{11}} & -\frac{\partial q_{01}}{\partial \psi_{10}} & 1 - \frac{\partial q_{01}}{\partial \psi_{01}} \end{vmatrix} = \begin{vmatrix} 1 + Cq_{11} & Cq_{11} & Cq_{11} \\ Cq_{10} & 1 + Cq_{10} & -Cq_{11} \\ Cq_{01} & -Cq_{11} & 1 + Cq_{01} \end{vmatrix} = (1 + C\psi)(1 - C\psi_{11}),$$

where first the derivatives of q_{ij} are calculated and then the conditions that $q_{11} = \psi_{11}$, $q_{10} = \psi_{10}$, etc., at the saddle point and $\psi = \psi_{10} + \psi_{11}$ are used to simplify the expression. Substituting the values for ψ and ψ_{11} for the saddle point gives

$$\langle\Omega^2\rangle = \langle\Omega^2\rangle_{\text{far}} + \langle\Omega^2\rangle_{\text{near}} = \frac{\langle\Omega\rangle^2}{\left(1 + W\left(-\frac{W^2(C)}{C}\right)\right)} + \frac{\langle\Omega\rangle}{1 - W^2\left(-\frac{W^2(C)}{C}\right)} \text{ for } C > C_{\text{crit}}.$$

These formulae give behavior at the transition that is very similar to the Kauffman model: when $C \approx e$, the mean number of fixed points is finite, $\langle\Omega\rangle \approx \frac{1}{2}$ and

$$\langle\Omega^2\rangle \approx \begin{cases} \frac{e}{2(e-C)} & \text{if } C < e \\ \frac{e}{C-e} & \text{if } C > e \end{cases}. \quad (\text{G8})$$

It is also interesting to consider the limit when C is large: For large C , $\langle\Omega\rangle = \frac{1}{1+W(C)} \approx \frac{1}{\ln C}$, which tends to zero. The second moment is approximately the same as the first moment, which can be understood if one assumes that it is very unlikely for their to be more than one fixed point. We have also calculated $\langle\Omega\rangle$ and $\langle\Omega^2\rangle$ when the model is modified so that loops are not allowed. The saddle point calculations are very similar to the case where loops are allowed: the saddle point has the same location, and there is a factor without singularities multiplying the expression. For the inhibitory model, we find that $\langle\Omega\rangle = \frac{C}{W(C)(1+W(C))}$. On the one hand, the extra factor of $\frac{C}{W(C)}$ is not singular at the transition point, so the qualitative behavior at the transition is not affected by whether loops are allowed. On the other hand, the limit at large C is different, $\langle\Omega\rangle \approx \frac{C}{(\ln C)^2}$, tending to infinity; when loops are allowed and C is large, many sites have edges to themselves, so they cannot be on at a FP, and this constraint rules out most possibilities for FPs and makes $\langle\Omega\rangle$ tend to zero instead.

Below the transition one can calculate the full distribution of Ω ; As for the Kauffman model, the probability of a fixed point existing tends to zero at C_{crit} .

3. Dynamics

Now we consider the dynamics briefly. The time dependence of the magnetization changes its behavior at C_{crit} . To see this, note that a fixed point ψ^* of $\psi \rightarrow q(\psi)$ is attractive if $|q'(\psi^*)| < 1$. Calculating $q'(\psi^*)$ from Eq. (G1) and the value of ψ^* , one sees that the derive $q'(\psi^*)$ is between -1 and 0 when $C < e$ and is less than -1 when $C > e$. Hence the fixed point begins to repel ψ when $C > e$. One can check that there is a 2-cycle that ψ is attracted to in this case.

On the other hand, the mean number of fixed points $\langle\Omega\rangle = \frac{1}{|1-q'(\psi^*)|}$ does not have any nonanalytic behavior at e . For one, $\psi^*(C) = W(C)/C$ varies analytically near $C = e$, and for two $q'(\psi^*) = -1$, so $\langle\Omega\rangle$ does not diverge.

Now consider the dynamics of $\vec{\psi} = (\psi_{11}, \psi_{10}, \psi_{01}, \psi_{00})$. We saw above that it has a unique fixed point, $(W(C)/C, 0, 0, 1 - W(C)/C)$, when $C < e$. This fixed point attracts all initial values of $\vec{\psi}$. This has a consequence for the dynamics of specific configurations: it implies that they are all attracted to a common fixed point (up to finitely many sites) since the distance between any two tends to $\psi_{10} + \psi_{01} = 0$. I.e., this is a frozen state. When $C > e$, this fixed point becomes unstable and $\vec{\psi}$ is attracted to 2-cycles instead (which agrees with the instability in the dynamics of the magnetization).

At the same C , there is also a transition in the FPs from one cluster to multiple clusters. Unlike for the Kauffman model, the distance between FPs in different clusters is not related to the value of $\psi_{10} + \psi_{01}$ for the steady-state value

of $\vec{\psi}$ that the system is attracted to. This does not even make sense, because $\vec{\psi}$ is not attracted to a steady-state but to 2-cycles! The distance between FPs from different clusters was found in Sec. G2 to be given by the value of $\psi_{01} + \psi_{10}$ at a second fixed point that appears at $C = e$. (This point is also unstable, but it still is important for the properties of the FPs.) These observations show that the transition in the dynamics and the transition in the properties of the fixed points could possibly happen at different C_{crit} 's (if the model is changed slightly). One transition is related to the appearance of the attractive 2-cycles and the other is related to the appearance of a fixed point with $\psi_{01} + \psi_{10} \neq 0$.

Appendix H: The sum for the Inhibitory Model

The sum $f(x) = \sum_{k_1, k_2=0}^{\infty} \frac{k_1^{k_2} k_2^{k_1}}{k_1! k_2!} x^{k_1+k_2} = \frac{1}{1-W(-x)^2}$ has an interesting analytical derivation, which we found with the help of an entry in the Online Encyclopedia of Integer Sequences [36] and advice from its author, Paul Hanna. The entry is about the sequence of numbers

$$a_n = \sum_{j=0}^n \binom{n}{j} j^{n-j} (n-j)^j.$$

This integer is essentially the sequence of coefficients of $f(x)$: After substituting $n = k_1 + k_2$ and $j = k_1$ in the definition of $f(x)$, $f(x) = \sum_{j=0}^n \frac{a_n x^n}{n!}$. The article states the formula $f(x) = \frac{1}{1-W(-x)^2}$ (due to Paul Hanna). The proof is not given but the formula can be derived from another interesting formula for a_n given in the article (due to Vladeta Jovovic [36]) :

$$\frac{a_n}{n!} = \frac{n^n}{n!} - \frac{n^{n-1}}{(n-1)!} + \frac{n^{n-2}}{(n-2)!} - \dots + \frac{(-1)^n}{0!}. \quad (\text{H1})$$

So first let us prove Eq. H1 and then derive the formula for $f(x)$. We begin with

$$n! = \sum_{j=0}^n (-1)^{n-j} \binom{n}{j} (\sigma + j)^n, \quad (\text{H2})$$

where σ can be any number. This can be found in books about the calculus of finite differences: Define the difference operator on a function, $\Delta g(\sigma) = g(\sigma + 1) - g(\sigma)$. By calculating the differences of the differences iteratively, $\Delta^k \sigma^n$ is a polynomial whose degree is $n - k$ and whose leading coefficient is $n(n-1)(n-2) \dots (n-k+1)$, for $k \leq n$. If $k = n$, this means $\Delta^n \sigma^n$ is a constant and the constant is $n!$ The operator Δ can be written as $D - I$ where D is a shift operator, $Dg(\nu) = g(\nu + 1)$, so $\Delta^n = \sum_{j=0}^n (-1)^{n-j} \binom{n}{j} D^j$ by the binomial theorem. So $\Delta^n \sigma^n = n!$ is the same as Eq. (H2).

Now substitute this formula into the definition of a_n :

$$\begin{aligned} a_n &= \sum_{j=0}^n \binom{n}{j} j^{n-j} \left[\sum_{k=0}^j \binom{j}{k} n^k (-j)^{j-k} \right] \\ &= \sum_{0 \leq k \leq j \leq n} (-1)^{j-k} \binom{n-k}{j-k} \binom{n}{n-k} j^{n-k} n^k \\ &= \sum_{0 \leq l \leq s \leq n} (-1)^l \binom{s}{l} \binom{n}{s} (l+n-s)^s n^{n-s} \\ &= \sum_{s=0}^n (-1)^s \binom{n}{s} s! n^{n-s}. \end{aligned}$$

The third step changed variables to $s = n - k$ and $l = n - j$, and the last step used Eq. (H2). This is the same as Eq. (H1)

Now this can be substituted into $f(x)$ and summed using the Taylor series for $W(x)$.

$$f(x) = \sum_{d=0}^{\infty} (-1)^d \sum_{n=d}^{\infty} \frac{n^{n-d} x^n}{(n-d)!}.$$

Now $W(x)^d = \sum_{n=d}^{\infty} (-1)^{n-d} d \frac{n^{n-d-1} x^n}{(n-d)!}$ (see Ref. [31], Eq. 2.36) and differentiating with respect to x gives $\frac{W(x)^d}{(1+W(x))} = \sum_{n=d}^{\infty} (-1)^{n-d} \frac{n^{n-d} x^n}{(n-d)!}$ (using Eq. (B3)). Hence

$$f(x) = \sum_{d=0}^{\infty} \frac{W(-x)^d}{1+W(-x)} = \frac{1}{1-W(-x)^2}.$$

- [1] Marc Mézard, Giorgio Parisi, and Miguel Virasoro. *Spin Glass Theory and Beyond: An Introduction to the Replica Method and Its Applications*, volume 9. World Scientific Publishing Co. Inc., 1987.
- [2] S. A. Kauffman. Metabolic stability and epigenesis in randomly constructed genetic nets. *Journal of Theoretical Biology*, 22(3):437–467, March 1969.
- [3] Stuart Kauffman. Homeostasis and differentiation in random genetic control networks. *Nature*, 224(5215):177–178, 1969.
- [4] John J. Hopfield. Neural networks and physical systems with emergent collective computational abilities. *Proceedings of the national academy of sciences*, 79(8):2554–2558, 1982.
- [5] Charles K. Fisher and Pankaj Mehta. The transition between the niche and neutral regimes in ecology. *PNAS*, 111(36):13111–13116, September 2014.
- [6] B Derrida. Dynamical phase transition in nonsymmetric spin glasses. *J. Phys. A: Math. Gen.*, 20(11):L721–L725, August 1987.
- [7] U. Bastolla and G. Parisi. Relevant elements, magnetization and dynamical properties in Kauffman networks: A numerical study. *Physica D: Nonlinear Phenomena*, 115(3):203–218, May 1998.
- [8] James F. Lynch. On the threshold of chaos in random Boolean cellular automata. *Random Structures & Algorithms*, 6(2-3):239–260, 1995.
- [9] B. Derrida and G. Weisbuch. Evolution of overlaps between configurations in random Boolean networks. *J.de Physique*, 47:1297, 1986.
- [10] B. Derrida and H. Flyvbjerg. Distribution of local magnetisations in random networks of automata. *J. Phys. A*, 20:L1107, 1987.
- [11] Stuart A. Kauffman. Metabolic stability and epigenesis in randomly constructed genetic nets. *Journal of theoretical biology*, 22(3):437–467, 1969.
- [12] U. Bastolla and G. Parisi. The modular structure of Kauffman networks. *Physica D*, 115:219, 1997.
- [13] J.E.S. Socolar and S.A. Kauffman. Scaling in ordered and critical random Boolean networks. *Physical Review Letters*, 90:068702, 2003.
- [14] Björn Samuelsson and Carl Troein. Superpolynomial growth in the number of attractors in kauffman networks. *Physical Review Letters*, 90(9):098701, 2003.
- [15] Konstantin Klemm and Stefan Bornholdt. Stable and unstable attractors in Boolean networks. *Physical Review E*, 72(5):055101, November 2005.
- [16] Florian Greil and Barbara Drossel. Dynamics of critical Kauffman networks under asynchronous stochastic update. *Physical Review Letters*, 95(4):048701, July 2005.
- [17] Peter Krawitz and Ilya Shmulevich. Basin entropy in Boolean network ensembles. *Physical Review Letters*, 98(15):158701, April 2007.
- [18] Viktor Kaufman, Tamara Mihaljev, and Barbara Drossel. Scaling in critical random Boolean networks. *Physical Review E*, 72:046124, 2005.
- [19] Tamara Mihaljev and Barbara Drossel. Scaling in a general class of critical random Boolean networks. *Phys. Rev. E*, 74:046101, 2006.
- [20] T. M. A. Fink and F. C. Sheldon. Number of attractors in the critical kauffman model is exponential. *Phys. Rev. Lett.*, 131:267402, Dec 2023.
- [21] Yael Fried, Nadav M. Shnerb, and David A. Kessler. Alternative steady states in ecological networks. *Phys. Rev. E*, 96:012412, July 2017.
- [22] Julio Aracena. Maximum number of fixed points in regulatory Boolean networks. *Bulletin of Mathematical Biology*, 70:1398, 2008.
- [23] B Derrida and Y Pomeau. Random networks of automata: A simple annealed approximation. *Europhys. Lett.*, 1(2):45–49, January 1986.
- [24] Béla Bollobás. *Random Graphs*. Number 73 in Cambridge Studies in Advanced Mathematics. Cambridge University Press, Cambridge; New York, 2nd edition, 2001.
- [25] H. Flyvbjerg. An order parameter for networks of automata. *J. Phys. A: Math. Gen.*, 21:L955, 1988.
- [26] H. Flyvberg. Recent results for random networks of automata. *Acta Physica Polonica B*, 20(4):321.
- [27] Boris Pittel, Joel Spencer, and Nicholas Wormald. Sudden emergence of a giant k-core in a random graph. *Journal of Combinatorial Theory, Series B*, 67:111, 1996.
- [28] Tobias Johnson, Moumanti Podder, and Fiona Skerman. Random tree recursions: Which fixed points correspond to tangible sets of trees? *Random Structures and Algorithms*, 56:796, 2020.
- [29] F. Greil and B. Drossel. Kauffman networks with threshold functions. *Eur. Phys. J. B*, 57:109–113, 2007.

- [30] Ari M. Turner. Fixed points of networks with sparse connections: The hybrid method (in preparation).
- [31] R.M. Corless, G.H. Gonnet, D.E.G. Hare, D.J. Jeffrey, and D.E. Knuth. On the Lambert W function. *Advances in Computational Mathematics*, 5:326, 1996.
- [32] Z.A. Melzak. *Companion to Concrete Mathematics*. John Wiley and Sons, New York, 1st edition, 1973.
- [33] G. Pólya and R.C. Read. *Combinatorial Enumeration of Groups, Graphs, and Chemical Compounds*. Springer Verlag, New York, 1st ed. edition, 1987.
- [34] László Lovász. *Combinatorial Problems and Exercises*. AMS Chelsea Publishing, Providence, 2nd edition, 2007.
- [35] Noga Alon and Joel H. Spencer. *The Probabilistic Method*. John Wiley and Sons, New York, 2nd ed. edition, 2000.
- [36] Paul D. Hanna. Online Encyclopedia of Integer Sequences, sequence A134095. <https://oeis.org/A134095>.